HHS Public Access

Author manuscript

*Biomaterials*. Author manuscript; available in PMC 2019 April 01.

Published in final edited form as:

*Biomaterials*. 2018 April ; 161: 240–255. doi:10.1016/j.biomaterials.2018.01.006.

# Dual non-viral gene delivery from microparticles within 3D high-density stem cell constructs for enhanced bone tissue engineering

**Alexandra McMillan**[a], **Minh Khanh Nguyen**[b], **Tomas Gonzalez-Fernandez**[c,d,e,f], **Peilin Ge**[b], **Xiaohua Yu**[g,h], **William Murphy**[g,h,i], **Daniel J. Kelly**[c,d,e,f], and **Eben Alsberg**[b,j,k,l,*]

[a]Pathology, Case Western Reserve University, 10900 Euclid Ave. Cleveland, OH 44106, USA [b]Biomedical Engineering, Case Western Reserve University, 10900 Euclid Ave. Cleveland, OH 44106, USA [c]Trinity Centre for Bioengineering, Trinity Biomedical Sciences Institute, Trinity College Dublin, Ireland [d]Department of Mechanical and Manufacturing Engineering, School of Engineering, Trinity College Dublin, Ireland [e]Advanced Materials and Bioengineering Research Centre (AMBERG), Trinity College Dublin and Royal College of Surgeons in Ireland [f]Tissue Engineering Research Group, Dept. of Anatomy, Royal College of Surgeons in Ireland, Dublin, Ireland [g]Department of Biomedical Engineering, University of Wisconsin-Madison, Madison, WI, USA [h]Department of Orthopedics and Rehabilitation, University of Wisconsin-Madison, Madison, WI, USA [i]Materials Science Program, University of Wisconsin-Madison, Madison, WI, USA [j]Orthopaedic Surgery, Case Western Reserve University, 10900 Euclid Ave. Cleveland, OH 44106, USA [k]The National Center for Regenerative Medicine, Case Western Reserve University, 10900 Euclid Ave. Cleveland, OH 44106, USA [l]School of Dentistry, Kyung Hee University, Seoul, South Korea

## Abstract

High-density mesenchymal stem cell (MSC) aggregates can be guided to form bone-like tissue via endochondral ossification in vitro when culture media is supplemented with proteins, such as growth factors (GFs), to first guide the formation of a cartilage template, followed by culture with hypertrophic factors. Recent reports have recapitulated these results through the controlled spatiotemporal delivery of chondrogenic transforming growth factor-β1 (TGF-β1) and chondrogenic and osteogenic bone morphogenetic protein-2 (BMP-2) from microparticles embedded within human MSC aggregates to avoid diffusion limitations and the lengthy, costly in vitro culture necessary with repeat exogenous supplementation. However, since GFs have limited stability, localized gene delivery is a promising alternative to the use of proteins. Here, mineral-coated hydroxyapatite microparticles (MCM) capable of localized delivery of Lipofectamine-plasmid DNA (pDNA) nanocomplexes encoding for TGF-β1 (pTGF-β1) and BMP-2 (pBMP-2)

*Corresponding author. Department of Biomedical Engineering, Case Western Reserve University, 10900 Euclid Ave, Cleveland, OH 44106, USA. Tel.: 1 216 368 6425; eben.alsberg@case.edu.

were incorporated, alone or in combination, within MSC aggregates from three healthy porcine donors to induce sustained production of these transgenes. Three donor populations were investigated in this work due to the noted MSC donor-to-donor variability in differentiation capacity documented in the literature. Delivery of pBMP-2 within Donor 1 aggregates promoted chondrogenesis at week 2, followed by an enhanced osteogenic phenotype at week 4. Donor 2 and 3 aggregates did not promote robust glycosaminoglycan (GAG) production at week 2, but by week 4, Donor 2 aggregates with pTGF-β1/pBMP-2 and Donor 3 aggregates with both unloaded MCM and pBMP-2 enhanced osteogenesis compared to controls. These results demonstrate the ability to promote osteogenesis in stem cell aggregates through controlled, non-viral gene delivery within the cell masses. These findings also indicate the need to screen donor MSC regenerative potential in response to gene transfer prior to clinical application. Taken together, this work demonstrates a promising gene therapy approach to control stem cell fate in biomimetic 3D condensations for treatment of bone defects.

### Keywords

Hydroxyapatite; Mesenchymal stem cells; Bone regeneration; Scaffold-free constructs; Endochondral ossification; TGF-β1; BMP-2

## Introduction

Critical-sized bone defects, caused by trauma, infection, tumor resection, or congenital disorders, are marked by impaired regenerative capacity, preventing healing during the course of a patient's lifetime [1]. The current gold standard for treatment of these defects is bone autografts, which are limited by supply, geometry, size, and donor site morbidity [2]. Allografts are an alternative, but have been associated with disease transmission and immune rejection [3]. Bone tissue engineering strategies offer the potential to provide regenerative tissue to treat critical-sized bone defects without the aforementioned limitations. In these approaches, cells are often used in combination with biomaterials, soluble biochemical signals and/or physical stimuli to direct cell behavior. Mesenchymal stem cells (MSCs) are widely utilized in engineering skeletal tissues [4] because they are readily available from the bone marrow, undergo self-renewal, and have the capacity to differentiate down multiple lineages including the chondrogenic, osteogenic, and adipogenic pathways. MSCs can be seeded onto or within 3D scaffolds, along with incorporated growth factors (GFs) or genes, to promote their differentiation into osteoblasts capable of producing new bone matrix [5–9]. However, scaffold-based approaches require matching scaffold degradation with new tissue formation [10], have potential toxicity due to synthesis techniques or degradation by-products, may interfere with mechanotransduction signaling to cells via stress-shielding [11], and may hinder cell-cell interactions present during native development [12, 13].

Scaffold-free approaches involve cell-cell adhesion molecule-mediated self-assembly into high- density cell condensations in a variety of geometric forms, such as aggregates and sheets, with the capacity to overcome limitations associated with scaffolds [11, 12]. Importantly, stem cell condensations have been shown to undergo both chondrogenic and

osteogenic differentiation [13–18], typically through the addition of specific proteins in the culture medium. GFs of the transforming growth factor-β (TGF-β) family, such as TGF-β1, have been used for chondrogenesis [13, 19] and bone morphogenetic proteins (BMPs), such as BMP-2, have been used for both chondrogenesis and osteogenesis [20–22]. In particular, BMP-2 has been shown to promote chondrocyte proliferation and hypertrophy, an integral step in endochondral ossification [23], one of two bone formation pathways that occur during native long bone formation and fracture healing. As opposed to bone regeneration by intramembranous ossification, in which MSCs directly differentiate into osteoblasts, stem cells in the endochondral ossification pathway first differentiate into chondrocytes that form a cartilaginous anlage which is then ultimately remodeled into bone [24]. Chondrocytes have low metabolic requirements, potentially leading to enhanced survival of cells within the constructs when implanted in vivo. Additionally, hypertrophic chondrocytes within the anlage secrete angiogenic factors that recruit blood vessels and regenerative cells, providing an intrinsic mechanism to promote vascular invasion of the implant [25–27]. These features make endochondral ossification a desirable differentiation pathway for bone engineering.

Strategies to drive endochondral ossification in MSC aggregates have primed cells with chondrogenic GFs to first create a hypertrophic cartilage template that can then be remodeled to form bone by culture in hypertrophic medium, osteogenic medium, and/or in vivo implantation [14, 26, 28–30]. For example, Scotti et al. engineered bone by culturing scaffold-free hMSC sheets for 3 weeks with TGF-β1 to induce chondrogenesis, culturing for an additional 2 weeks in hypertrophic medium supplemented with β-glycerophosphate and L-thyroxine, a hormone that promotes hypertrophy, followed by subcutaneous implantation in mice [26]. Constructs developed a cartilage matrix core surrounded by a bony collar. Alternatively, Farrell et al. demonstrated that culture of hMSC condensations with chondrogenic medium supplemented with TGF-β2, to initiate hypertrophy and secretion of angiogenic factors, followed by a switch to medium supplemented with β-glycerophosphate resulted in mineralization of the constructs [29]. Although high-density cell constructs supplied with exogenous GFs have achieved chondro-osseous differentiation, this mode of delivery increases the time needed before constructs can be implanted. Further, diffusion limitations may decrease GF presentation to cells on the interior, leading to non-homogenous differentiation. Our lab has circumvented issues of exogenous GF delivery and demonstrated the capacity to drive both cartilage and bone formation via incorporation of GF-laden microparticles within 3D hMSC condensations [31–37]. Gelatin microparticles (GM) loaded with TGF-β1 and mineral coated hydroxyapatite (HA) microparticles (MCM) loaded with BMP-2 were incorporated into high-density hMSC aggregates, resulting in endochondral ossification [31] and a system capable of regenerating cranial bone defects in rats [38]. Despite these promising findings, GF delivery may be limited by high cost and short half-life in vivo [39, 40].

Gene therapy has emerged as a powerful tool for programming target regenerative cells to produce chondroinductive and osteoinductive signals, while potentially avoiding protein stability problems [9, 41–43]. Gene delivery can be achieved by several methods, including viral and non-viral methods. Non-viral delivery approaches decrease issues of insertional mutagenesis and immunogenicity of viral vectors [44], but comes at the cost of transient expression and decreased transfection efficiency [45]. Regarding transgene expression in

MSC condensations, plasmid DNA (pDNA) delivery to cells in monolayer culture prior to 3D aggregate formation has been reported [46]. However, the short-term nature of a single administration of pDNA offers little control over the duration of expression [47], thus limiting the extent of protein presentation during the time course of differentiation [40]. Biodegradable materials can be of great use to locally deliver and control presentation of genetic material to nearby cells to promote healing [40]. In addition to sustained presentation of pDNA from biomaterials, gene delivery within 3D constructs has been demonstrated to enhance transfection efficiency of non-viral vectors [40, 48, 49]. For example, MSCs in a 3D collagen sponge exhibited a 4-fold increase in pDNA-derived BMP-2 expression compared to 2D monolayer transfection [49]. Therefore, sustained presentation of GF-encoded genetic material from microparticles within high-density cell condensations may circumvent the transiency of one-time pDNA dosing and enhance efficacy of non-viral vectors compared to 2D culture.

In this work, we hypothesized that MCM-bound Lipofectamine-complexed pDNA expressing TGF-β1 (pTGF-β1) and BMP-2 (pBMP-2), alone or in combination, could be locally delivered from within porcine MSC aggregates to promote endochondral ossification. This strategy would overcome limitations of GF delivery and one-time pDNA dosing. The MCM serve as both an osteoconductive signal, by providing a mineral source [31], and also a means to locally deliver pTGF-β1 and pBMP-2 within a 3D stem cell environment capable of expressing and responding to produced GF. This pDNA-bound microparticle system provides the first proof-of principle platform for the sustained delivery of genetic material within cellular condensations to induce the production of GFs involved in the complex process of endochondral ossification and drive bone formation.

## Methods

### Experimental design

The aim of the work described here was to investigate the potential to deliver bioactive pDNA encoding GFs from MCM incorporated in porcine MSC aggregates to direct endochondral ossification. Three healthy porcine donors were used to examine how donor-to-donor variability can affect gene expression, GF production profiles, and differentiation in this system. First, MSC aggregates containing cells only or unloaded MCM (MCM alone) were cultured sequentially in chondrogenic and then osteogenic medium supplemented with exogenous TGF-β1 and BMP-2, respectively, to study the role of these exogenous signals and MCM on endochondral ossification in this system. Biochemical, histological, and immunohistochemical markers of differentiation were evaluated at 2 and 4 weeks. To assess pDNA-mediated GF production over time in 2D monolayer MSC culture, cells were treated with a single dose of Lipofectamine-complexed pDNA encoding TGF-β1 and BMP-2, and GF levels were analyzed over time. pDNA encoding TGF-β1 and BMP-2, in isolation or combination, was then bound to MCM and introduced into aggregates to determine the capacity of this system to transfect MSCs and induce GF production over time in 3D culture. Transgene incorporated aggregates were cultured for 2 weeks in chondrogenic medium followed by 2 weeks in osteogenic medium to promote differentiation into bone-like tissue via remodeling of a cartilage template. Biochemical, histological, and immunohistochemical

markers of differentiation were assessed at 2 and 4 weeks. The cytocompatibility of the pDNA-MCM particles was assessed by DNA quantification at weeks 2 and 4.

### Porcine MSC isolation and expansion

Porcine bone marrow-derived MSCs were obtained from three porcine donors. Briefly, MSCs were isolated from the femora of 3–4 month-old female Danish duroc pigs (40–45 kg) via density gradient centrifugation and differential cell adhesion to tissue culture plastic as previously described [9, 50]. Adherent cells (MSCs) were cultured in growth medium consisting of high-glucose Dulbecco's Modified Eagle's Medium Glutamax (DMEM-HG; Sigma-Aldrich, St. Louis, MO) with 10% fetal bovine serum (FBS, Sigma-Aldrich) and 1% penicillin/streptomycin (P/S, MP Biomedicals, Solon, OH). Beyond passage 1, medium was supplemented with 10 ng/mL fibroblast growth factor-2 (FGF-2, R&D Systems, Minneapolis, MN) and expanded to passage 3–4. All cell culture took place at 37°C with 5% $CO_2$ in a humidified incubator.

### MCM synthesis

Hydroxyapatite (HA) microparticles were prepared as previously described [51]. HA microparticles, between 3–5 μm in diameter, were obtained from Plasma Biotal LTD (Derbyshire, UK) and mineral-coated in modified simulated body fluid (mSBF) with 2 times (2×) the concentration of calcium and phosphate of human blood plasma. Briefly, HA microparticles were added at 2 mg/ml to mSBF (pH 6.8) containing 141 mM NaCl, 4.0 mM KCL, 0.5 mM $MgSO_4$, 1.0 mM $MgCl_2$, 20.0 mM HEPES, 5.0 mM $CaCl_2$, 2.0 mM $KH_2PO_4$, and 4.2 mM $HaHCO_3$. The mSBF was stirred at 37°C for 7 days with fresh mSBF replaced daily. The particles were then rinsed with di$H_2O$ and lyophilized.

### Exogenous growth factor supplementation of cells only and MCM alone aggregates

Basal pellet medium (BPM) consisting of DMEM-HG supplemented with 1% $ITS^+$ Premix (Corning Inc, Corning, NY), 1% sodium pyruvate (GE Healthcare Life Sciences, Logan, UT), 1% P/S, 40 mg/ml L-proline (Sigma-Aldrich), 50 mg/ml L-ascorbic acid-2-phosphate (Wako Chemicals USA Inc., Richmond, VA), 4.7 μg/ml linoleic acid (Sigma-Aldrich), and 1.5 mg/ml bovine serum albumin (Sigma-Aldrich) was used as the base medium for chondrogenic and osteogenic medium. Chondrogenic medium consisted of BPM supplemented with 100 nM dexamethasone (MP Biomedicals). Osteogenic medium consisted of BPM supplemented with 1 nM dexamethasone, 10 mM β-glycerophosphate (EMD Millipore, MA, USA), and 1 nM L-thyroxine (Sigma-Aldrich). Cells only and unloaded microparticle-incorporated MSC aggregates were formed in a manner similar to that previously described [31]. Briefly, MSCs were trypsinized and suspended with or without 0.03 mg MCM per aggregate at a concentration of $2.5 \times 10^5$ cells/mL in chondrogenic medium, and 1 ml was dispensed into 1.5 ml Eppendorf tubes (Fisher Scientific). Constructs were cultured in 1 ml of media, as opposed to the 200 μl of medium used by our lab in previous studies [31], to create a lower oxygen tension environment, which has been shown to favor MSC chondrogenesis in vitro [52, 53]. The tubes were centrifuged at 650 g for 5 min to form aggregates, and the medium was changed every other day.

Cells only and MCM alone aggregates from three MSC donors were treated with exogenous GF (cells only with exoGF and MCM alone with exoGF, respectively) and cultured in chondrogenic medium supplemented with 10 ng/ml TGF-β1 (PeproTech, Rocky Hill, NJ) for two weeks followed by culture in osteogenic medium supplemented with 100 ng/ml BMP-2 (Dr. Walter Sebald, Department of Developmental Biology, University of Würzburg, Germany) for two weeks to demonstrate endochondral ossification in porcine MSCs using the described culture setup. Aggregates were harvested at 2 and 4 weeks and stored at −20°C for biochemical analysis (N=3 aggregates per condition per time point), or in 10 % neutral buffered formalin at 4°C for histology (N=2 aggregates per condition per time point), as described below.

### Plasmid DNA-vehicle formation and monolayer transfection

MSCs were transfected in monolayer with pDNA to assess cell-specific GF production. One day before transfection, MSCs were plated into 6-well plates (Fisher Scientific, Pittsburgh, PA) in growth medium of DMEM-HG with 10% FBS and 1% P/S, at a density of $1\times10^5$ cells/well and cultured for 24 hours (hrs). On the day of transfection, MSCs were treated with 1 μg/well of DNA (pTGF-β1, Sinobiological, Beijing, China, or pBMP-2, a generous gift from Chris Evans, Harvard Medical School [43]) complexed with Lipofectamine 2000 (Fisher Scientific) for 6 hrs. Lipofectamine was complexed with pDNA according to the manufacturer's instructions at a ratio of 2:1 of Lipofectamine (μl): DNA (μg) in PBS, and the solution was then incubated for 15 minutes (min) at room temperature (RT) for complex formation followed by suspension in DMEM-HG for transfection. All pDNA used in this work was complexed with Lipofectamine at a 2:1 ratio. After 6 hrs the medium was replaced with fresh growth medium. Cell culture medium was collected at defined time points, replaced with fresh growth medium, and stored at −80°C prior to ELISA analysis (N=3). The average concentration of baseline BMP-2 or TGF-β1 produced by untreated cells was subtracted from pBMP-2 or pTGF-β1 treated wells, respectively, at each time point. GF was quantified using ELISAs according to the manufacturer's instructions (R&D, Minneapolis, MN) with the absorbance of each sample read at 450 nm using a microplate reader (Molecular Devices, Sunnyvale, CA). 540 nm readings were subtracted from 450 nm values to account for optical imperfections in the plate and analyzed against a standard curve using 4-Parameter Logistic (4PL) curve fitting.

### Plasmid DNA loading and binding efficiency to MCM

A schematic of the process employed to form Lipofectamine-pDNA bound MCM is shown in Fig. 1A. MCM were loaded with Lipofectamine-pDNA complexes which were prepared as described above. Microparticles suspended in di$H_2O$ at 10 mg/ml were loaded with the Lipofectamine-pDNA solution by rotation for 2 hrs at RT to allow for binding (2 μg pDNA per 0.03 mg MCM). The solution was centrifuged (Thermoscientific Survall Legend RT + Centrifuge, Fisher Scientific) at 2,000 g for 5 min, and the supernatant was removed to obtain only MCM with bound pDNA nanocomplexes. The binding efficiency of Lipofectamine-pDNA expressing green fluorescent protein (pGFP; Clontech, Mountain View, CA) to MCM (N=3) was determined by quantifying unbound pGFP in the supernatant. Supernatant was collected and mixed with 10 mg/ml heparin (20 μl supernatant with 10 μl heparin) for 20 min to dissociate the plasmid complex, and the concentration of

DNA in the supernatant was measured using the Picogreen assay kit (Life Technologies) at $\lambda_{ex}/\lambda_{em}$ = 485/538 nm to determine the total unbound DNA (N=3). Values were compared to a standard curve of Lipofectamine-complexed pGFP also treated with heparin.

### MCM incorporation efficiency within MSC aggregates

The incorporation efficiency of MCM in aggregates was determined by forming MSC aggregates with cells only or by incorporating 0.03 mg MCM alone or with 2 μg of bound Lipofectamine-pGFP per aggregate (2 μg pDNA per 0.03 mg MCM; 0.03 mg MCM per aggregate). Briefly, MSCs were trypsinized and suspended alone, or with unloaded or pDNA-loaded MCM, at a concentration of $2.5 \times 10^5$ cells/mL in chondrogenic medium, and 1 ml was dispensed into 1.5 ml Eppendorf tubes (Fisher Scientific). The tubes were centrifuged at 650 g for 5 min to form aggregates. MSC aggregates were cultured for 3 days in chondrogenic medium with exogenous TGF- β1 (10 ng/ml), harvested, and digested in papain buffer overnight for analysis of calcium and DNA content (N=4 aggregates per condition), as described below. Incorporation efficiency was determined by calculating the ratio of total calcium per aggregate to the theoretical input of 12 μg calcium from 0.03 mg of MCM. DNA was analyzed to determine the short-term effect of pDNA delivery on cell viability. DNA content of 2 μg Lipofectamine-pDNA bound to MCM was analyzed with the same protocol used to assess cellular DNA content of aggregates to determine if Lipofectamine-pGFP/MCM incorporation in the aggregates impacts measured cellular DNA content. To determine whether MCM distributed homogenously within the aggregates and to serve as a comparison for mineralization of constructs at later time points, MCM alone aggregates were also cultured for 3 days in chondrogenic medium, harvested in 10 % neutral buffered formalin for histological processing (N=2 aggregates), and stained for calcium with Alizarin Red S (ARS, Sigma-Aldrich).

### Short-term determination of transgene produced GF retained in aggregate and secreted

MSC aggregates incorporating MCM alone, pTGF-β1-, pBMP-2-, or pTGF-β1/pBMP-2-loaded MCM, were formed in a manner similar to that described above. Briefly, Donor 1 MSCs were trypsinized and suspended with MCM alone or with pDNA bound MCM (2 μg DNA per 0.03 mg MCM; 0.03 mg MCM per aggregate) at a concentration of $1.25 \times 10^6$ cells/mL, and 200 μl was dispensed per well into sterile 96-well V-bottom polypropylene microplates (Fisher Scientific). The plates were centrifuged at 500 g for 5 min to form aggregates. 200 μl was used here due to the ease of handling 96-well plates compared to 1.5 mL Eppendorf tubes used in the differentiation studies. All aggregates with incorporated plasmid in this work received 2 μg of pDNA in total. 2 μg of pDNA was incorporated per aggregate in pTGF-β1 and pBMP-2 groups, whereas 1 μg of each plasmid was incorporated in the pTGF-β1/pBMP-2 group. Medium (secreted portion) was collected at day 3, and aggregates (bound portion) were harvested and stored at −80°C. Prior to ELISA analysis, aggregates were thawed and added to a 1 ml solution of 1 M ethylenediaminetetraacetic acid (EDTA, Fisher Scientific) and 9% ammonium hydroxide at pH 7.1 followed by homogenization (35,000 rpm, Omni International, Marietta, GA) and incubation for 2 hrs at 37°C. The levels of produced BMP-2 and TGF-β1 were quantified using ELISAs according to the manufacturer's instructions as previously described (N=3). Baseline BMP-2 or TGF-

β1 values produced by cells only aggregates were not subtracted from experimental conditions.

### Plasmid DNA-MCM incorporated aggregate formation for long-term determination of GF production and MSC differentiation

Cells only, microparticles alone, and microparticles loaded with pTGF-β1, pBMP-2, or pTGF-β1/pBMP-2 were incorporated within MSC aggregates in the same manner as described in the MCM incorporation efficiency section ($2.5 \times 10^5$ MSCs per Eppendorf tube; 2 μg pDNA total per 0.03 mg MCM; 0.03 mg MCM per aggregate). The medium was changed every other day and collected for ELISA analysis (N=3). Culture medium was collected every two days at medium changes up to day 16. Medium was pooled between days 0–4, 5–8, 9–12, and 13–16 and analyzed via ELISA as described above. Baseline BMP-2 or TGF-β1 values produced by cells only aggregates were not subtracted from experimental conditions. Aggregates were maintained in chondrogenic medium for 2 weeks followed by 2 weeks in osteogenic medium for biochemical and histological analysis at weeks 2 and 4, as described below. For each individual donor, the aforementioned aggregates were formed and cultured in the same experiment as aggregates supplemented with exoGF.

### Quantitative biochemical analysis

Aggregates were harvested at 2 and 4 weeks and assayed for DNA, glycosaminoglycan (GAG) and calcium content, and alkaline phosphatase (ALP) activity (N=3 aggregates per condition per time point) according to a previously reported protocol [31]. Briefly, aggregates were homogenized twice for 30 s on ice in 1 ml papain buffer (Sigma-Aldrich, 35,000 rpm). ALP lysis buffer (1 mM $MgCl_2$, 20 μm $ZnCl_2$ and 0.1 % octyl-β-glucopyranoside in 10 mM Tris buffer at pH 7.4) was added to half of each sample. ALP activity was measured using an ALP assay kit (Sigma-Aldrich) according to the manufacturer's instructions and compared to a standard curve of *para*-nitrophenol (Sigma-Aldrich) after a 30 min incubation with *para*-nitrophenylphosphate (pNPP, Sigma-Aldrich) at 37°C using a plate reader at 405 nm. ALP activity is expressed as amounts of converted substrate read from the *para*-nitrophenol standard curve (μM). The other half of each sample was digested overnight in papain buffer at 65°C. The next day, an aliquot of this sample was treated with 1M HCl to dissolve MCM, and assayed for calcium content using an *o*-cresophthalein complexone assay (Sigma-Aldrich) and a standard curve prepared with calcium analyzed using a plate reader at 570 nm. The remainder of the aliquot was used to quantify GAG and DNA. The sample was treated with 10% EDTA in 0.05 M Tris-HCl buffer (pH7.4) to dissociate DNA from the MCM and centrifuged at 1000 g for 5 min for analysis of the supernatant. DNA analysis was performed with the Picogreen assay kit. GAG was measured with dimethyl-methylene blue (DMMB, Sigma-Aldrich) at an absorbance of 595 nm.

### Histological and immunohistochemical analysis

After 2 and 4 weeks of culture, all aggregate conditions were harvested and fixed overnight in 10 % neutral buffered formalin and paraffin-embedded. Mounted tissue sections (10 μm thick) were stained for sulfated GAG via Safranin-O (SafO, Acros Organics, Fisher

Scientific) with Fast Green counterstain (Fisher Scientific), calcium with ARS, and hematoxylin (Fisher HealthCare, Fisher Scientific) and eosin (Richard-Allan Scientific, ThermoFisher Scientific, Waltham, MA) (H&E). Immunohistochemistry (IHC) was performed on aggregates to analyze the presence of collagen types I, II and X (col I, II, X). Histology sections were deparaffinized and rehydrated with decreasing concentrations of ethanol, and endogenous peroxidase activity was quenched with 30% vol/vol hydrogen peroxide/methanol (1:9) for 10 min. Protease (1mg/ml; Sigma-Aldrich) was applied to each section at RT for 30 min for epitope retrieval. Anti-col I (1:250, ab138492), anti-col II (1:200, ab34712), and anti-col X (1:200, ab49945) (Abcam, Cambridge, MA) were used as primary antibodies and detected with Histostain-Plus kit via 3-Amino-9-ethylcarbazole (AEC, Fisher Scientific) according to the manufacturer's instructions. Slides were counterstained with 1% Fast Green and cover slip mounted with glycerol vinyl alcohol (Invitrogen). Images were acquired on an Olympus BX61VS microscope (Olympus, Center Valley, PA, USA) with a Pike F-505 camera (Allied Vision Technologies, Stadtroda, Germany) (N=2 aggregates per condition per time point). Sections presented in the figures are from samples that exhibited the most extensive SafO staining and chondrocyte morphology at 2 and 4 weeks. Sections were randomly chosen for conditions that did not demonstrate extensive chondrogenic differentiation.

### Aggregate sizing

Freshly harvested aggregates (N=4) from Donors 2 and 3 were imaged using a Galaxy S4 phone camera (Samsung, Seoul, Korea) with a ruler in each image for size calibration. The diameter of each aggregate was obtained by averaging measurements (12 to 6, 2 to 8, and 4 to 10 o'clock) from two independent researchers using ImageJ software (NIH, Washington, DC).

## Statistical analysis

Results were presented as means (± standard deviation) for each condition. Statistical analyses were performed using one-way ANOVA with post-hoc Tukey analysis with GraphPad Prism software (La Jolla, CA). $p$ values less than 0.05 were considered statistically significant.

## Results

### Endochondral ossification of cells only and MCM alone aggregates with exogenous growth factor supplementation

Cells only and aggregates with unloaded MCM were cultured with exoGF to examine the capacity of the porcine MSC aggregates to undergo endochondral ossification when cultured for 2 weeks in TGF-β1-supplemented chondrogenic medium followed by 2 weeks in BMP-2-supplemented osteogenic medium.

**Cell content—**DNA content of aggregates was analyzed to assess cell viability and proliferation. Average DNA content at weeks 2 and 4 was less than 1.5 μg in both groups, the total theoretical amount present in the $2.5 \times 10^5$ cells used to form each aggregate

(assuming ~6 pg of DNA per nucleus [54]). No significant differences were observed in DNA content between cells only with exoGF and MCM alone with exoGF aggregates harvested at 2 and 4 weeks for each of the donors (Supp. 1A,B,C). By week 4, average DNA content decreased in all donors, but no significant differences were observed between the two time points in Donor 1 and 3 aggregates. Both Donor 2 cells only with exoGF and MCM alone with exoGF aggregates resulted in significantly lower DNA content relative to week 2 values.

**GAG content—**Since GAGs are a primary component of cartilage extracellular matrix [55], GAG content was evaluated as an indicator of cartilage formation at weeks 2 and 4. Cells only with exoGF aggregates produced significantly greater GAG relative to MCM alone with exoGF aggregates at weeks 2 and 4 for all donors with the exception of Donor 3, in which cells with exoGF aggregates had similar GAG content compared to MCM alone with exoGF at week 2 (Supp. 1D,F,H). GAG content of Donor 2 cells only with exoGF and MCM alone with exoGF aggregates significantly increased from week 2 to 4 (Supp. 1F).

**ALP activity—**ALP activity was then measured as it is expressed by hypertrophic chondrocytes and is an early marker of osteogenesis [56, 57]. Supplementation of Donor 1 and 3 cells only with exoGF aggregates resulted in significantly higher ALP activity at 2 weeks compared to MCM alone with exoGF aggregates (Supp. 1J,N), while there were no differences between these groups in Donor 2 (Supp. 1L). By week 4, ALP activity of constructs from all donors with exoGF was significantly decreased compared to week 2, and no differences were observed between conditions at this time point.

**Calcium content—**When MSCs differentiate into osteoblasts, the osteoblasts lay down osteoid matrix which is subsequently mineralized with calcium-containing bone apatite [58]. Therefore, calcium content in the constructs was analyzed as an indicator of bone formation. Calcium content in cells only with exoGF constructs at 2 weeks for all donors was minimal, while that for MCM alone with exoGF constructs approached the amount of calcium that was initially incorporated into aggregates from MCM-derived calcium, assuming 100% incorporation efficiency (Supp. 1P,R,T). By week 4, both groups with exoGF had significantly increased calcium content compared to week 2, with no significant differences between conditions at this time point for all donors.

**Histology: Donor 1—**SafO staining was used to examine the presence and spatial distribution of GAG, a marker of cartilage formation. IHC was performed to stain for col II, which is found within articular cartilage [59], and col X, a marker for hypertrophic cartilage [60]. Week 2 Donor 1 cells only with exoGF and MCM alone with exoGF aggregates resulted in intense SafO and col II staining in a similar pattern in both conditions, with evidence of hypertrophic chondrocytes (Supp. 2A,C). Col X was present in cells only with exoGF aggregates while none was present in the MCM alone with exoGF aggregates (Supp. 2C). In addition to cartilage markers, ARS staining was used to examine for the presence of calcium, an indicator of mineralization and bone formation [58]. IHC for col I, the predominant collagen found in bone [59], was also examined as a marker of osteogenic differentiation. When cultured with exogenous GFs, cells only aggregates did not stain with

ARS, but calcium was present within the interior of the MCM-incorporated aggregates (Supp. 2A). Col I exhibited a similar pattern with SafO staining in cells only with exoGF aggregates. MCM alone with exoGF stained more intensely for col I than cells only with exoGF, with staining throughout the aggregates (Supp. 2C).

Four weeks after culture in sequential chondrogenic and then osteogenic medium, samples were examined histologically for changes in cartilage marker expression. Delivery of exoGF to cells only and MCM alone aggregates resulted in intense, homogenous staining for SafO with distinct chondrocytic and hypertrophic morphology (Supp. 2B). Col II and X stained intensely on the periphery of cells only with exoGF aggregates and less intensely in the core. Both groups resulted in intense col II staining, with more homogenous staining throughout MCM alone with exoGF aggregates than cells only with exoGF aggregates. Similarly, col X staining was more homogenous throughout the MCM with exoGF than cells with exoGF group, although col X stained less intensely compared to col II (Supp. 2D). With regard to osteogenic markers of differentiation, MCM alone with exoGF aggregates demonstrated intense staining for calcium with ARS stain, while cells only with exoGF aggregates showed mineralization only at the periphery (Supp. 2B). Staining for col I resulted in staining at the periphery of cells only with exoGF aggregates and more homogenously throughout the MCM alone with exoGF aggregates (Supp. 2D).

**Histology: Donor 2—**After 2 weeks, Donor 2 aggregates (Supp. 3A) cultured with exoGF stained uniformly for SafO. Col II was present on the periphery of cells only with exoGF aggregates (Supp. 3C), while MCM alone with exoGF aggregates stained more uniformly for this chondrogenic marker. Both exoGF groups showed evidence of hypertrophic morphology (Supp. 3A), although col X was not present in week 2 aggregates (Supp. 3C). Calcium staining was not detected at 2 weeks in the cells only with exoGF aggregates but stained the periphery of MCM alone with exoGF aggregates (Supp. 3A). Col I was faintly present at week 2 at the periphery of cells only with exoGF aggregates and throughout MCM alone with exoGF aggregates (Supp. 3C).

By week 4, the intense, homogenous staining for SafO exhibited by week 2 cells only with exoGF and MCM alone with exoGF aggregates was still evident (Supp. 3B). Col II was present throughout the cells only with exoGF aggregates and more intensely throughout the MCM alone with exoGF group (Supp. 3D). Col X was present in both groups at week 4 (Supp. 3D). Calcium staining in both Donor 2 exoGF groups was homogenous (Supp. 3B). Col I stained throughout both the cells only and MCM alone with exoGF groups, although more intense staining was present in the latter group (Supp. 3D).

**Histology: Donor 3—**Both Donor 3 exoGF aggregates conditions stained strongly throughout for SafO and col II at week 2 (Supp. 4A,C). More intense staining of col II was observed in the MCM alone with exoGF condition. No col X was present at week 2 in either exoGF groups (Supp. 4C). Both exoGF conditions also stained intensely for col I at week 2 (Supp. 4C) with more intense staining in the MCM with exoGF condition. No calcium was evident in cells only with exoGF aggregates at week 2, but the MCM alone with exoGF condition demonstrated calcium staining irregularly distributed within the aggregates (Supp. 4A).

By week 4, both conditions cultured with exoGF continued to stain intensely for SafO, but MCM alone with exoGF aggregates were less homogenously stained (Supp. 4B). There was intense staining for both col II and X at week 4 in both exoGF conditions (Supp. 4D), which was increased compared to week 2. Calcium distributed towards the periphery of the cells only with exoGF aggregates, while the MCM alone with exoGF condition stained homogenously throughout (Supp. 4B). Intense staining for col I was observed at week 4 in both exoGF conditions (Supp. 4D).

### TGF-β1 and BMP-2 pDNA induced GF production in monolayer cultured MSCs

To investigate plasmid derived production of TGF-β1 and BMP-2 over time in 2D culture, monolayer Donor 1 MSCs were transfected with Lipofectamine-complexed pDNA encoding for TGF-β1 and BMP-2, respectively. Lipofectamine-pTGF-β1 transfection exhibited the capacity to induce MSC secretion of TGF-β1 for a sustained period of at least 10 days, with a maximum average production at day 5 (Fig. 2A). BMP-2 production from MSCs treated with pBMP-2, on the other hand, was not sustained beyond day 3 (Fig. 2B), producing approximately 5 % of the maximum protein at day 3 compared to pDNA derived TGF-β1 at day 5.

### MCM incorporation into aggregates and pDNA binding efficiency to MCM

Incorporation of unloaded MCM within MSC condensations resulted in distribution of MCM throughout the constructs, with increased presence at the periphery of the cell condensations at day 3 (Supp. 5A), as demonstrated by calcium staining with ARS. Binding efficiency of pDNA complex to MCM was quantified as 76.5 ± 4.4 % and incorporation efficiency of microparticles alone or with 2 μg bound pDNA in Donor 1 aggregates, measured as aggregate calcium content, was 120.7 ± 2.11 % and 78.6 ± 6.2 %, respectively (Supp. 5B). The greater than 100 % incorporation efficiency is likely a result of compounded technical error of weighing and pipetting small amounts and volumes, respectively. Cellular DNA content was measured as a combined indicator of cell incorporation into the aggregates along with viability and proliferation after 3 days with incorporation of 2 μg pDNA (theoretical) compared to cells only and MCM alone aggregates (Supp. 5C). There was no statistical difference between the conditions. It should be noted that 2 μg pDNA complexed with Lipofectamine and bound to MCM results in measured DNA of 0.31 ± 0.07 μg using the Picogreen assay. Thus, the total DNA value for the pDNA bound to MCM conditions is likely the sum of the total cellular DNA in aggregate and a portion of the incorporated pDNA. Calcium/DNA values of these aggregates showed the same trend seen with calcium content (Supp. 5D).

### MCM loaded with pTGF-β1 and/or pBMP-2 incorporated into cell aggregates can transfect MSCs and induce production of TGF-β1 and/or BMP-2, respectively

After demonstrating that MSCs in monolayer culture could produce TGF-β1 or BMP-2 after treatment with pTGF-β1 or pBMP-2, respectively, and capacity for pDNA to bind MCM, pDNA-bound MCM were incorporated into Donor 1 MSC aggregates to evaluate the capacity for cell condensations to take up pDNA and express GF. Aggregates incorporating pTGF-β1 harvested at day 3 of culture produced 1043.6 pg/ml TGF-β1 (Fig. 2C), which was significantly higher compared to MCM alone, pBMP-2, and dual delivery aggregates. Dual

delivery of pTGF-β1/pBMP-2 also resulted in significantly greater TGF-β1 secretion compared to MCM alone and pBMP-2 aggregates. Both pTGF-β1 and pTGF-β1/pBMP-2 aggregates demonstrated minimal retention of the TGF-β1 within the aggregate (bound). MCM alone and pBMP-2 groups expressed negligible secreted and bound TGF-β1. Aggregates incorporated with pBMP-2-loaded MCM produced approximately 10-fold less BMP-2 in the medium compared to pTGF-β1-produced TGF-β1, but BMP-2 was found to be retained within the aggregates at similar quantities compared to secreted GF (Fig. 2D). Quantification of secreted and bound BMP-2 was significantly greater in both the pBMP-2 only and dual delivery aggregates compared to negligible BMP-2 produced by MCM alone and pTGF-β1 aggregates. pBMP-2 aggregates produced significantly more total BMP-2 relative to all other groups.

### Demonstration of sustained transgene expression in MSC aggregates

Once successful uptake and protein production of transgenes delivered from MCM within the MSC aggregates was achieved, the potential for the system to drive sustained secretion of the encoded proteins was examined. Aggregates from 3 different donors were formed with cells only, unloaded MCM, and MCM loaded with pTGF-β1 and/or pBMP-2 and cultured for 2 weeks in chondrogenic medium followed by 2 weeks in osteogenic medium to promote endochondral ossification. Quantification of TGF-β1 in the culture medium from Donor 1 aggregates incorporating pTGF-β1 demonstrated production of 1147.4 pg/ml TGF-β1 after 4 days, which was significantly more than all other groups at that time point (Fig. 3A). However, TGF-β1 production was not sustained beyond day 4. Co-delivery of pTGF-β1 and pBMP-2 did not result in significantly increased TGF-β1 relative to control aggregates. Donor 2 aggregates incorporated with pTGF-β1 produced more TGF-β1 than cells only, MCM alone, pBMP-2, and dual delivery aggregates at day 4 and sustained production to day 8 relative to cells only and MCM alone controls (Fig. 3B). The co-delivery group, incorporating pTGF-β1/pBMP-2, demonstrated sustained TGF-β1 production relative to cells only and pBMP-2 aggregates to day 16. Single delivery of pTGF-β1 in Donor 2 aggregates produced less than half the amount of TGF-β1 compared to the same Donor 1 condition at day 4. Donor 2 co-delivery aggregates showed longer term production of TGF-β1 compared to Donor 1 co-delivery aggregates. Similar to Donors 1 and 2, Donor 3 aggregates exhibited significantly greater TGF-β1 production in pTGF-β1 aggregates compared to all other groups at day 4 (Fig. 3C). No TGF-β1 was produced beyond the first time point. Dual delivery aggregates also had elevated TGF-β1 production between days 0–4 compared to all groups, except pTGF-β1 aggregates, with no significant GF production detected beyond this time point.

Donor 1 aggregates incorporating pBMP-2 alone and combination pTGF-β1/pBMP-2 resulted in sustained secretion of BMP-2 that was significantly greater than all other groups between 0–4, 5–8, and 9–12 days of culture (Fig. 4A). The pBMP-2 group produced 5.5 % of the level of TGF-β1 production in the pTGF-β1 group by day 4. BMP-2 production in the pBMP-2 and co-delivery groups was similar at all time points. Donor 2 pBMP-2 aggregates resulted in sustained production to at least day 16 (Fig. 4B). Day 4 BMP-2 production was significantly greater than cells only, MCM alone, and pTGF-β1 aggregates and significantly greater than all groups at the subsequent time points. BMP-2 production from the co-

delivery group was significantly higher than the cells only, MCM alone, and TGF-β1 groups, but it was not sustained beyond this time point. In comparison to Donor 1 pBMP-2 aggregates, Donor 2 pBMP-2 aggregates demonstrated more sustained BMP-2 production (Fig. 4B), but Donor 2 co-delivery aggregates did not sustain production to the same extent as Donor 1 aggregates of the same condition. Donor 3 pBMP-2 aggregates sustained BMP-2 production to day 12, and production was greater than all other groups at day 4 and greater than MCM alone aggregates at days 8 and 12 (Fig. 4C). Donor 3 pBMP-2 aggregates had a similar BMP-2 expression profile compared to Donor 1 pBMP-2 aggregates. Dual delivery aggregates' production of BMP-2 was greater than all groups with the exception of pBMP-2 aggregates at day 4, but it was not sustained compared to Donor 1 dual-delivery aggregates.

### pDNA enhanced chondrogenesis and calcification for endochondral ossification

To determine the influence of pTGF-β1 and/or pBMP-2 delivery on endochondral ossification in porcine MSC condensations, the same aggregates for which sustained GF production was quantified were assessed for chondrogenic and osteogenic differentiation. To evaluate the extent of differentiation, aggregates from all donors were analyzed for DNA, GAG content, alkaline phosphatase (ALP) activity, and calcium content at 2 and 4 weeks. Additionally, chondrogenic and osteogenic markers were investigated via histological analysis in all donors. Immunohistochemical analysis of Donor 1 and 3 aggregates assessed the qualitative amount and distribution of proteinaceous markers of differentiation. Since pDNA-incorporated aggregates and aggregates cultured with exoGF received different concentrations and temporal presentation of GFs, pDNA-incorporated aggregates are presented separately in this section. Biochemical results of pDNA-incorporated aggregates relative to aggregates supplemented with exoGF are presented in the Supplemental material (Supp. 1).

**Cell content—**To assess the role of MCM and/or pDNA delivery on cell viability and proliferation, aggregate DNA content was measured. Similar to aggregates cultured with exogenous GF, average DNA content at weeks 2 and 4 was less than the theoretical incorporation of 1.5 μg DNA per aggregate. No significant differences were observed in DNA content between Donor 1 groups harvested at 2 weeks, or between groups at 4 weeks (Fig. 5A). By week 4, average DNA content decreased, but no significant differences were observed between the two time points with the exception of pBMP-2 aggregates. Similarly, Donor 2 groups did not show significant differences amongst conditions within weeks 2 or 4 or between time points (Fig. 5B), with the exception of pBMP-2 aggregates, which had lower cell content by week 4. DNA content of Donor 3 aggregates did not show significant differences amongst conditions within weeks 2 or 4 or between time points (Fig. 5C).

**GAG content—**The produced GAG content in Donor 1 pBMP-2 aggregates at 2 weeks was significantly higher than that of MCM alone, pTGF-β1, and pTGF-β1/pBMP-2 aggregates and exhibited higher average GAG content compared to all other groups (Fig. 5D). GAG content decreased by week 4 in pBMP-2 and dual delivery aggregates. Donor 2 aggregates did not show significant GAG differences at weeks 2 or 4, although co-delivery resulted in higher average GAG content at week 2 compared to all other groups (Fig. 5E). Donor 3 aggregates did not show significantly different GAG values between conditions at

week 2 (Fig. 5F). GAG values in cells only, MCM alone, and dual-delivery aggregates increased by week 4. pTGF-β1 and pBMP-2 aggregates had higher GAG content at this time point relative to cells only aggregates.

When GAG was normalized to DNA, similar GAG/DNA values were observed between Donor 1 conditions at 2 weeks, and no change was observed over time with the exception of an increase in GAG/DNA in pTGF-β1 aggregates by week 4 (Supp. 6A). At 4 weeks, GAG/DNA values of pTGF-β1 aggregates were significantly higher than all other conditions. Donor 2 pTGF-β1 aggregates demonstrated significantly increased GAG/DNA values over time, and week 4 values were significantly higher compared to the MCM alone, pBMP-2 and pTGF-β1/pBMP-2 aggregates (Supp. 6B). Donor 3 GAG/DNA values were not significantly different between groups or time points with the exception of pTGF-β1 aggregates, which demonstrated increased GAG/DNA values at week 4 relative to week 2. pTGF-β1 aggregates' week 4 values were greater compared to cells only, MCM alone, and pBMP-2 aggregates (Supp. 6C).

**ALP activity—**Only the pBMP-2 group in Donor 1 aggregates expressed substantial ALP activity at week 2, which was significantly greater compared to all groups (Fig. 5G). pBMP-2 aggregates' ALP activity decreased precipitously by week 4 to comparably low levels observed in the other groups at both time points. Donor 2 aggregates incorporating pTGF-β1/pBMP-2 showed a significantly higher ALP activity at week 2 relative to all other groups, which then also significantly decreased to low levels by week 4 (Fig. 5H). Donor 3 ALP activity was low and not significantly different between conditions at week 2, but by week 4, MCM aggregates' ALP activity was greater than all other conditions (Fig. 5I).

There were no significant differences in ALP/DNA values between Donor 1 groups at each time point or within a condition over time with the exception of pBMP-2 aggregates which had significantly higher values compared to all other groups at week 2 followed by a significant decrease by week 4 (Supp. 6D). Donor 2 aggregates incorporating pTGF-β1/pBMP-2 showed significantly higher ALP/DNA (Supp. 6E) at week 2 relative to all other groups, which then decreased by week 4. Donor 3 ALP/DNA values were not significantly different between conditions at week 2, but by week 4, MCM alone aggregates resulted in significantly increased ALP/DNA relative to week 2 and all other conditions (Supp. 6F). pBMP-2 aggregates had significantly higher ALP/DNA relative to pTGF-β1 and dual delivery aggregates at week 4.

**Calcium content—**Measured calcium values at 2 weeks in all donors (Fig. 5J,K,L) were lower than the input from the incorporated MCM (12 μg calcium as represented by the dashed line), indicating that minimal calcification took place during this period of culture in chondrogenic medium. Calcium content of Donor 1 pBMP-2 aggregates significantly increased between weeks 2 and 4 and was significantly higher at the latter time point compared to cells only, MCM alone, and pTGF-β1/pBMP-2 aggregates, indicating mineralization (Fig. 5J). Donor 2 pBMP-2 and co-delivery aggregates contained significantly higher calcium than aggregates containing cells only at week 2 (Fig. 5K). By week 4, MCM alone, pBMP-2, and pTGF-β1/pBMP-2 aggregates had significantly greater calcium content compared to cells only aggregates, with dual delivery aggregates' calcium

being significantly greater compared to week 2 and to all other groups. Donor 3 MCM alone and dual delivery aggregates had significantly increased calcium content relative to cells only aggregates at week 2 (Fig. 5L). By week 4, both MCM alone and pBMP-2 aggregates had significantly increased calcium, which was higher compared to cells only, pTGF-β1, and pTGF-β1/pBMP-2 aggregates.

When normalized to DNA content, no significant differences were observed between Donor 1 groups at weeks 2 and 4, although pTGF-β1 calcium/DNA values increased over time, likely as a result of lower average DNA values at week 4 (Supp. 6G). Donor 2 pTGF-β1 aggregates had significantly higher calcium/DNA values at week 4 compared to week 2 aggregates, also likely as a result of lower average DNA. At week 4, this group had significantly higher values relative to all other groups (Supp. 6H). Calcium/DNA values in Donor 3 aggregates were not significantly different between conditions at week 2, but by week 4, pTGF-β1 and pBMP-2 aggregates' values were significantly increased and higher compared to cells only aggregates (Supp. 6I).

**Histology: Donor 1—**Donor 1 aggregates were assessed with SafO, ARS, and H&E as well as col II, I, and X as markers of chondrogenic and osteogenic differentiation. Histological sections from Donor 1 week 2 aggregates were first stained for chondrogenic markers (Fig. 6A). Strikingly, cells in the pBMP-2 aggregates developed a round, chondrocytic morphology within lacunae surrounded by a homogenous GAG-rich matrix with presence of both regular and hypertrophic chondrocytes. The engineered tissue for the cells only, pTGF-β1, and pTGF-β1/pBMP-2 aggregates displayed moderate presence of GAG, but without the chondrocytic cellular morphology. MCM alone aggregates stained only minimally for GAG. Homogenous col II staining was present throughout the pBMP-2 group (Fig. 7A), consistent with the accumulation of GAG. Cells only, MCM alone, pTGF-β1, and pTGF-β1/pBMP-2 aggregates also stained for col II but less intensely than pBMP-2 aggregates. None of these groups stained for col X, except for faint staining in the pTGF-β1 aggregates.

Along with markers for cartilage formation, evidence of bone formation was also examined at week 2. pBMP-2 aggregates stained positively for calcium predominantly at the construct periphery (Fig. 6A). Calcium was also observed in all other conditions, with the exception of cells only aggregates, in a similar distribution but with slightly more intense staining compared to pBMP-2 aggregates. This ARS staining is likely representative of the residual incorporated MCM present at week 2 and/or low-level bone-like neomineralization (Fig. 5J). Day 3 MCM alone aggregates stained intensely for calcium (Supp. 5A), providing a comparison for the remodeling and bone formation that occurs at later time points. IHC staining for col I demonstrated heterogenous distribution within pBMP-2 aggregates (Fig. 7A). All other groups did not stain for col I.

Four weeks after culture in sequential chondrogenic and then osteogenic medium, samples were again examined histologically for markers of differentiation. With regard to chondrogenic markers, Donor 1 pBMP-2 samples displayed less GAG staining compared to week 2, indicating loss or remodeling of cartilage matrix (Fig. 6B). This group also demonstrated a non-homogenous, SafO-positive GAG matrix embedded with cells

presenting both a normal chondrogenic phenotype and also larger, round cells, providing evidence of hypertrophic chondrocytes. The other groups stained minimally for GAG, with cells only aggregates exhibiting more SafO staining compared to MCM alone, pTGF-β1, and pTGF-β1/BMP-2 aggregates. Compared to week 2 pBMP-2 aggregates, week 4 aggregates stained more intensely but less homogenously for col II (Fig. 7B). Although MCM alone aggregates did not yield rigid constructs, col II was present in the remaining tissue. Col II was also present in the cells only, pTGF-β1, and dual delivery aggregates, with intense, homogenous staining in the cells only group. Minimal col X staining was present in all groups at this time point.

Staining of week 4 aggregates was also performed to confirm the presence of bone-like tissue. Intense calcium was found in pBMP-2 aggregates along with the other MCM containing groups (Fig. 6B). Col I was present in a heterogeneous distribution in pBMP-2 aggregates (Fig. 7B). Interestingly, the cells only group demonstrated intense pockets of col I staining with some hypertrophic chondrocyte morphology distributed within a rich col II matrix. MCM aggregates demonstrated presence of col I, while both pTGF-β1 and pTGF-β1/pBMP-2 aggregates stained minimally to none for this protein. Some col X was present in pBMP-2 aggregates in patches, and there was faint staining in the other groups (Fig. 7B).

**Histology: Donor 2—**Donor 2 aggregates were assessed with SafO, ARS, and H&E to examine cartilage and bone formation. Week 2 pBMP-2 and pTGF-β1/pBMP-2 aggregates displayed centrally located GAG staining with presence of chondrocytes and some larger, hypertrophic chondrocytes (Supp. 7A). No GAG was present in the other groups. The cells only group exhibited little positive calcium staining, while in the MCM alone, pTGF-β1, pBMP-2, and pTGF-β1/pBMP-2 groups, calcium presented at the periphery of the aggregates. By week 4, although no SafO or chondrocytic morphology was evident, all aggregates stained throughout for calcium with the exception of the cells only group (Supp. 7B).

**Histology: Donor 3—**Donor 3 aggregates were also assessed with SafO, ARS, and H&E, and additionally, col II, I, and X were examined as proteinaceous markers of chondrogenic and osteogenic differentiation. pBMP-2 and pTGF-β1/pBMP-2 aggregates displayed SafO staining within the interior of the aggregates at week 2 (Supp. 8A). No SafO was present in the other groups. However, col II was present in all conditions (Supp. 9A). Col X stained intensely in cells only aggregates, faintly at the periphery of MCM alone aggregates, and faintly throughout the remaining conditions. Calcium staining at week 2 was observed in all conditions containing MCM (Supp. 8A). Col I was present in both the dual delivery and MCM alone aggregates (Supp. 9A). The remaining aggregates did not stain for col I.

By week 4, no GAG staining was evident in any group (Supp. 8B). Col II was present throughout all conditions at week 4 (Supp. 9B), and there was minimal col X in all conditions. All MCM containing groups stained for calcium with intense staining present in the interior of the aggregates, with the exception of pBMP-2 aggregates (Supp. 8B). MCM alone aggregates stained more intensely for col I compared to 2 weeks and compared to all other groups at this time point (Supp. 9B). Additionally, cells only and dual delivery

aggregates stained non-homogenously for col I, while pTGF-β1 and pBMP-2 aggregates did not show evidence of col I staining.

**Sizing of exoGF and pDNA-incorporated aggregates—**On gross visual inspection, constructs from all donors cultured with exoGF grew larger over 4 weeks of culture. Donor 1 pBMP-2 and Donor 2 pTGF-β1/pBMP-2 aggregates grew larger over 4 weeks of culture compared to the other groups cultured without exoGF, indicative of extracellular matrix production. No pDNA incorporated Donor 3 aggregates resulted in discernable differences in size on gross examination relative to cells only and MCM alone aggregates. Measurements of aggregate diameters were taken from macroscopic images of Donor 2 (Supp. 10A) and 3 (Supp. 10B) constructs. Although the size of aggregates cultured with exoGF are not directly comparable to pDNA-incorporated aggregates due to differences in GF quantity and temporal presentation, it was observed that Donor 2 cells only with exoGF, MCM alone with exoGF, and dual delivery aggregates were significantly larger compared to cells only and MCM alone aggregates at week 2. pTGF-β1 and pBMP-2 aggregates were larger than cells only aggregates. By week 4, cells only with exoGF aggregates significantly increased in size relative to week 2 and were also significantly larger than all other groups. MCM alone with exoGF aggregates were significantly larger than cells only, MCM alone, pTGF-β1, and pBMP-2 aggregates. pTGF-β1 aggregates were significantly larger compared to cells only, and the pTGF-β1/pBMP-2 group was significantly larger relative to cells only, MCM alone, and pBMP-2 aggregates. With regard to Donor 3 aggregates, pBMP-2 aggregates at week 2 were larger than cells only, and dual delivery aggregates were significantly larger than all groups with the exception of those cultured with exoGF. Cells only with exoGF aggregates were significantly larger than all other groups at week 2 with the exception of MCM alone with exoGF aggregates, which were significantly larger than cells only, MCM alone, and pTGF-β1 aggregates. By week 4, both pBMP-2 and pTGF-β1/pBMP-2 aggregates were significantly larger than cells only and pTGF-β1 aggregates. Cells only with exoGF aggregates were significantly larger than all groups, and MCM alone with exoGF aggregates were significantly larger than cells only, MCM alone, pTGF-β1, and pBMP-2 aggregates.

## Discussion

Here, we propose a bone engineering strategy focused on recapitulating native cellular condensation, the first phase of chondrogenic differentiation during endochondral ossification, and controlling the presentation of bioactive signals inherent to the process within these condensations. It was first demonstrated that sequential presentation of exogenous chondrogenic GF, TGF-β1, followed by the chondrogenic and osteogenic GF, BMP-2, drove the endochondral ossification process within porcine MSC condensations. Although promising results were achieved using recombinant GF delivery within this system, exogenous supplementation may increase the time needed before constructs can be implanted [31–34, 36, 38]. Since recombinant proteins are expensive [36] and suffer from short half-lives and rapid degradation in vivo [40], pDNA delivery and uptake by MSCs offers an alternative approach to instruct cells to produce target proteins without the harmful side effects that can occur when supraphysiologic dosages of GF are used to overcome

protein stability issues [61], potentially enhancing therapeutic outcomes. While delivery of non-viral genetic material from macroscopic biopolymer scaffolds to encapsulated or surrounding cells for upregulation of specific genes has been shown to enhance uptake efficiency compared to 2D transfection [40, 48], to date, no reports demonstrate delivery of genetic material within high-density MSC aggregates to regulate cell behavior. The overall purpose of this present study was to investigate the effects of MCM-mediated delivery of pDNA encoding TGF-β1 and BMP-2, alone or in combination, for directed differentiation of porcine MSC aggregates via the endochondral ossification pathway for bone tissue engineering.

Calcium phosphate (CaP)-based biomaterials have been widely used in bone engineering because of their similarity to the chemical composition of bone mineral and their osteoconductive and osteoinductive nature [62, 63]. CaP microparticles (MCM) may also provide a mineral source for bone tissue engineering strategies. Recombinant GF delivery to cells alone and MCM-incorporated MSC condensations not only provided evidence that sequential culture for two weeks in chondrogenic medium followed by two weeks in osteogenic medium can partially recapitulate endochondral ossification in vitro, but also permitted understanding of the effect of MCM on MSC differentiation. At two weeks, aggregates cultured with exoGF aggregates stained intensely for SaFO (Supp. 2A,3A,4A), indicating chondrogenic differentiation, the first phase of endochondral ossification [24]. The combination of elevated ALP activity at week 2 (Supp. 1J,L,N), extensive col X staining at week 4 (Supp. 2D,3D,4D), and enhanced calcium content of both exoGF conditions at week 4 relative to cells only and MCM alone aggregates suggests transition from chondrogenesis towards MSC hypertrophy and osteogenesis, the final phase of endochondral ossification. Interestingly, although the addition of MCM to aggregates cultured with exoGF resulted in decreased GAG content in Donor 1 and 2 aggregates at weeks 2 and 4 (Supp. 1D,F,H), aggregates cultured with exoGF from all donors incorporating MCM resulted in more homogenous col I and col X (Supp. 2D,3D,4D) staining at week 4 compared to cells only with exoGF aggregates, suggesting that MCM may enhance osteogenesis via the endochondral pathway. Overall, exogenous supplementation of GFs to both cells only and MCM incorporated aggregates promoted similar levels of calcification (Supp. 1P,R,T), indicating bone-like tissue formation.

The biomimetic coating on the MCM, consisting of carbonated hydroxyapatite, can potentially influence cell behavior as well as bind biological molecules, including GFs [51, 64] and pDNA [65, 66], via affinity interactions, allowing for sustained release of the bioactive factors. Dissolution of these CaP coatings with bound pDNA has been shown to have a direct relationship with pDNA release, allowing for sustained release of bound plasmid [65]. The CaP dissolution rate and subsequent pDNA release profile can be tailored by varying the mSBF composition used to form the coatings [65, 66]. In addition, cell seeding on 3D scaffolds with these CaP coatings with bound non-viral pDNA complexes has resulted in enhanced cell transfection efficiency compared to conventional transfection of cells on 2D tissue culture substrates [66]. CaP dissolution may offer the added benefit of calcium-mediated enhanced transfection efficiency [67]. Therefore, establishing a CaP coating on hydroxyapatite microparticles (MCM) with bound non-viral transgenes encoding

for chondrogenic and osteogenic GFs and encapsulating the pDNA-bound MCM within 3D cell aggregates may allow for sustained plasmid delivery and efficient transfection.

In view of the benefits of non-viral gene delivery from CaP coatings, MCM were incorporated within stem cell aggregates and visualized with calcium staining. Heterogeneous MCM incorporation was observed throughout day 3 aggregates (Supp. 5A), allowing for localized presentation of pDNA to MSCs capable of autocrine and paracrine signaling, without disruption of aggregate formation. MCM then redistributed towards the aggregate periphery and/or new immature bone-like tissue developed in this region by week 2 (Fig. 6A, Supp. 7A, 8A). Since less calcium was measured at 2 weeks compared to that theoretically incorporated from the MCM in all groups (Fig. 5J,K,L), it is likely that the microparticle CaP coating underwent degradation or MCM were extruded from the aggregate. In addition, because cells within the constructs are more likely to first come in contact with MCM-released plasmid, this system has the added advantage of potentially minimizing off-target effects of pDNA delivery to host cells when implanted in vivo. All pDNA-incorporated MSC aggregates were of a size (average diameters of 0.7 - 1.1 mm by week 4; Supp. 10) that allows for ease of manipulation upon potential implantation.

The impact of pTGF-β1-, pBMP-2-, and pTGF-β1/pBMP-2 incorporation within the aggregates on GF production and resultant chondrogenic and osteogenic differentiation capacity was then examined. Three different donors were studied due to extensively reported MSC donor-to-donor variability in gene expression [68] and differentiation potential [29, 69–71]. GF production from Donor 1, 2, and 3 pBMP-2 aggregates demonstrated BMP-2 production to at least day 12 when pBMP-2 was delivered alone (Fig. 4). The long-term production of BMP-2 indicates the ability of the MCM to sustain production of this GF when compared to single administration monolayer transfection (Fig. 2B). BMP-2 has previously been shown to bind via charge interactions to CaP mineral coatings, acting as a sustained repository for the GF while also serving to stabilize it and preserve bioactivity [72]. Therefore, the observed extended presentation of pDNA-produced BMP-2 in this system may potentially be a result of BMP-2 retention within the MCM-incorporated aggregate, as observed at day 3 (Fig. 2D). On the other hand, delivery of pTGF-β1 did not show retention within the aggregates at day 3 (Fig 2C). In accordance with this observation, delivery of pTGF-β1 alone resulted only in early, short-term TGF-β1 secretion into the media in all donors (Fig. 3A,B,C). Although binding of TGF-β1 to CaP coatings has not, to our knowledge, been reported, TGF-β1 interactions with pericellular matrix molecules have been demonstrated to play a major role in the GF's activity [73] via binding and sequestration [74–76]. Variation in TGF-β1 production profiles may be due to donor-dependent ECM production and subsequent differences in ECM-TGF-β1 interactions. Also, unlike with exogenously delivered recombinant GFs, cellular regulation has a role in plasmid derived GF production. For example, Fierro et al. [77] reported decreased lenti-viral expressed TGF-β1 production in supernatants of human MSCs compared to transduced cells expressing FGF-2, PDGF-β, and VEGF using the same vector backbone, suggesting that TGF-β1 production is regulated post-transcriptionally. It is also important to note that, in the case of pTGF-β1/pBMP-2 aggregates, a lower dose of each plasmid was delivered relative to each gene delivered in isolation, as in the pTGF-β1 and pBMP-2 aggregates, to keep the total pDNA loading constant between groups. This difference in gene dosage can affect the

GF production profiles along with potential crosstalk between GF-dependent signaling pathways [78]. For example, TGF-β1 production was more sustained in Donor 2 aggregates receiving pTGF-β1/pBMP-2 compared to pTGF-β1 aggregates of the same donor (Fig. 3B). The differing GF production profiles between donors and between single vs dual delivery aggregates indicate that the cellular response to delivery of pDNA encoding GFs in this system may be impacted by several factors including donor variability, retention by the MCM or ECM, post-transcriptional regulation, pDNA dosage, and interplay of GF signaling.

In addition to pDNA-mediated GF production, the degree of cell survival and differentiation within the three donor populations was investigated. First, delivery of genetic factors to MSC aggregates did not significantly affect the total measured DNA content upon formation (Supp. 5C). However, because the total DNA content for the pDNA-MCM incorporated aggregates is likely the sum of the total cellular DNA in aggregate and a portion of the incorporated pDNA, cellular DNA values may have been lower than the other groups, potentially due to Lipofectamine-mediated cytotoxicity. Average DNA then decreased over the culture period, but no significant differences in DNA were observed between groups by week 4 (Fig. 5A,B,C). The decrease in average DNA by 4 weeks in many of the conditions is potentially a result of culture with osteogenic and hypertrophic factors inducing chondrocyte hypertrophy and apoptosis [79]. Additionally, newly mineralized tissue may create a physical obstruction to diffusion of nutrients and oxygen in vitro [80], leading to cell death. Importantly, the delivery of therapeutic transgenes within the three donor populations resulted in varying degrees of chondrogenesis. Delivery of pBMP-2 to Donor 1 aggregates and both pBMP-2 and pTGF-β1/pBMP-2 in Donor 2 aggregates induced the development of chondrocyte morphology and SafO staining in week 2 constructs (Fig. 6A, Supp. 7A). The enhanced chondrogenesis observed in Donor 1 pBMP-2 and Donor 2 pTGF-β1/pBMP-2 aggregates coincided with greater ALP activity at week 2 compared to all other groups (Fig. 5G,H). This enhanced ALP activity suggests presence of osteoblasts and/or hypertrophic chondrocytes, the latter of which could be evidence of initiation of endochondral ossification. Donor 3 aggregates exhibited minimal ALP activity (Fig. 5I) in response to GF production, but pBMP-2 and pTGF-β1/pBMP-2 aggregates stained for SafO (Supp. 8A), suggesting chondrogenic differentiation with minimal or delayed hypertrophy/osteoblastic development in these conditions. As noted earlier, less calcium was measured in all donors compared to that theoretically incorporated from the MCM suggesting that minimal bone formation likely occurred by week 2.

By 4 weeks, different plasmid delivery conditions resulted in enhanced osteogenesis between the donors, with Donor 1 pBMP-2, Donor 2 pTGF-β1/pBMP-2, and both Donor 3 MCM alone and pBMP-2 aggregates best promoting new bone-like tissue compared to the other conditions. These groups showed enhanced calcium content (Fig. 5J,K,L) and more intense ARS staining relative to week 2 aggregates (Fig. 6A, Supp. 7A,8A). Osteogenesis was further demonstrated by the increased presence of col I staining in the Donor 1 pBMP-2 and cells only aggregates (Fig. 7B) as well as Donor 3 MCM aggregates (Supp. 9B). The decreased level of ALP activity observed in Donor 1 pBMP-2 and Donor 2 pTGF-β1/pBMP-2 aggregates is likely due to the rise and fall of ALP activity during the process of bone formation as osteoblasts mature. Despite increased ALP activity in Donor 3 MCM alone aggregates at week 4, the average level of ALP activity was reduced in comparison to

Donor 1 pBMP-2 and Donor 2 dual delivery aggregates at week 2. This observed ALP activity in Donor 3 coincides with the lack of hypertrophic chondrocyte morphology at week 2 and low total calcium content by week 4 (Fig. 5L). The finding that delivery of pBMP-2 promoted both enhanced GAG deposition and calcification in Donor 1 aggregates is corroborated by the noted chondrogenic and osteogenic role of BMP-2 [23, 81]. Interestingly, MCM was sufficient to induce osteogenesis in Donor 3 aggregates, potentially due to the osteoinductive nature of CaP and donor-specific response [31, 63]. The presence of col X in Donor 1 and 3 aggregates at 2 and 4 weeks (Fig. 7, Supp. 9) did not correlate with osteogenic differentiation by week 4, with the exception of Donor 1 pBMP-2 aggregates (Fig. 7B), suggesting that aggregates may be undergoing chondrogenesis and osteogenesis independently as opposed to differentiating via endochondral ossification. Differences observed between donors with regard to which pDNA delivery condition, in conjunction with an MCM-derived, mineral-rich culture environment, led to an enhanced osteogenic response are likely due to the aforementioned factors, including pDNA dose, type of transgene delivered, and the variability between each cell population's differentiation potential and capacity to take up pDNA and express the encoded proteins [82].

Although differences in GF dosages and temporal presentation of GFs between exoGF groups and transgene-incorporated aggregates make comparisons difficult, it is striking that Donor 1 pBMP-2 (Supp. 1J) and Donor 2 pTGF-β1/pBMP-2 aggregates (Supp. 1L) produced similar ALP levels and their average calcium values (Supp. 1P,R) approached those from aggregates supplemented with exoGF. A lower total amount of protein was capable of directing differentiation in pDNA-incorporated aggregates relative to exogenously supplied protein. For example, Donor 1 exoGF aggregates were supplied with approximately 5,800-fold more BMP-2 (700 ng over two weeks), compared to the amount of BMP-2 secreted by pBMP-2 aggregates (~119.2 pg over 16 days; Fig. 4A), and yet, calcium levels by week 4 were comparable to that achieved with exoGF (Supp. 1P). Despite possible GF retention within the aggregate or degradation in the culture medium, reducing measured GF production, it is likely that less total pDNA-derived GF than that supplied exogenously was capable of driving differentiation. These results suggest that therapeutic transgenes from MCM can provide a promising alternative to protein delivery.

To the best of our knowledge, this is the first report to examine the capacity of pDNA encoding for the GFs, TGF-β1 and BMP-2, in combination or isolation, delivered from microparticles incorporated within a 3D stem cell condensation to drive cartilage and bone formation. Different CaP compositions have been shown to regulate the release of GFs and pDNA from MCM [51, 65, 66], supporting the potential of tailoring pDNA release from the current system. Importantly, this system is versatile and may accommodate the delivery of a multitude of different genes and gene combinations in a 3D biomimetic microenvironment without the need for repeated bioactive factor supplementation in culture medium and extensive in vitro culture time prior to implantation. Variable GF production profiles between donor cell populations resulting from delivery of a single or combination of plasmids resulted in different cellular responses; Donor 1 pBMP-2 aggregates exhibited enhanced osteogenesis after 4 weeks in vitro culture relative to cells only aggregates while Donor 2 pTGF-β1/pBMP-2 aggregates and Donor 3 MCM and pBMP-2 aggregates

presented this response. Given these findings, it might be necessary to screen the response of individual patients' cells prior to clinical implementation.

## Conclusion

This study demonstrates the capacity of localized delivery of pDNA-loaded microparticles incorporated within high-density porcine stem cell constructs to induce bone formation via a cartilage intermediate reminiscent of the endochondral ossification pathway. Localized delivery of a single or combination of TGF-β1 and BMP-2-encoded transgenes from within the cell constructs achieved therapeutic levels of bioactive protein capable of directing stem cell differentiation. Delivering genetic material offers a cell-derived supply of instructive protein(s), which eliminates the need to supply GFs directly and avoids associated issues of short half-life, high cost, and rapid degradation. As non-viral pDNA expression is transient, its sustained delivery from microparticles may allow for longer-term expression to responsive cells for enhanced regulation of cell behavior, circumventing the need for repeat supplementation with the potential to decrease in vitro culture time prior to implantation of the cell constructs. Future studies will examine the potential of this system to repair critical-sized bone defects in vivo and also investigate the system's utility for engineering other tissues using different cell populations and pDNA encoding for application-specific genes.

## Supplementary Material

Refer to Web version on PubMed Central for supplementary material.

## Acknowledgments

The authors thank Amad Awadallah for providing histological services, Melanie Chetverikova for help with imaging and manuscript edits, and the National Institutes of Health (AR066193, AR063194) for supporting this work.

## References

1. Dimitriou R, Jones E, McGonagle D, Giannoudis PV. Bone regeneration: current concepts and future directions. BMC Med. 2011; 9:66. [PubMed: 21627784]
2. Amini AR, Laurencin CT, Nukavarapu SP. Bone tissue engineering: recent advances and challenges. Crit Rev Biomed Eng. 2012; 40(5):363–408. [PubMed: 23339648]
3. Ng J, Spiller K, Bernhard J, Vunjak-Novakovic G. Biomimetic approaches for bone tissue engineering. Tissue Eng Part B Rev. 2016
4. Brown PT, Handorf AM, Jeon WB, Li WJ. Stem cell-based tissue engineering approaches for musculoskeletal regeneration. Curr Pharm Des. 2013; 19(19):3429–45. [PubMed: 23432679]
5. Ho SS, Vollmer NL, Refaat MI, Jeon O, Alsberg E, Lee MA, Leach JK. Bone Morphogenetic Protein-2 Promotes Human Mesenchymal Stem Cell Survival and Resultant Bone Formation When Entrapped in Photocrosslinked Alginate Hydrogels. Adv Healthc Mater. 2016; 5(19):2501–2509. [PubMed: 27581621]
6. Davis HE, Case EM, Miller SL, Genetos DC, Leach JK. Osteogenic response to BMP-2 of hMSCs grown on apatite-coated scaffolds. Biotechnol Bioeng. 2011; 108(11):2727–35. [PubMed: 21656707]
7. Simmons CA, Alsberg E, Hsiong S, Kim WJ, Mooney DJ. Dual growth factor delivery and controlled scaffold degradation enhance in vivo bone formation by transplanted bone marrow stromal cells. Bone. 2004; 35(2):562–9. [PubMed: 15268909]

8. Nguyen MK, Jeon O, Krebs MD, Schapira D, Alsberg E. Sustained localized presentation of RNA interfering molecules from in situ forming hydrogels to guide stem cell osteogenic differentiation. Biomaterials. 2014; 35(24):6278–86. [PubMed: 24831973]
9. Gonzalez-Fernandez T, Tierney EG, Cunniffe GM, O'Brien FJ, Kelly DJ. Gene Delivery of TGF-beta3 and BMP2 in an MSC-Laden Alginate Hydrogel for Articular Cartilage and Endochondral Bone Tissue Engineering. Tissue Eng Part A. 2016; 22(9–10):776–87. [PubMed: 27079852]
10. Alsberg E, Kong HJ, Hirano Y, Smith MK, Albeiruti A, Mooney DJ. Regulating bone formation via controlled scaffold degradation. J Dent Res. 2003; 82(11):903–8. [PubMed: 14578503]
11. DuRaine GD, Brown WE, Hu JC, Athanasiou KA. Emergence of scaffold-free approaches for tissue engineering musculoskeletal cartilages. Ann Biomed Eng. 2015; 43(3):543–54. [PubMed: 25331099]
12. Athanasiou KA, Eswaramoorthy R, Hadidi P, Hu JC. Self-organization and the self-assembling process in tissue engineering. Annu Rev Biomed Eng. 2013; 15:115–36. [PubMed: 23701238]
13. Johnstone B, Hering TM, Caplan AI, Goldberg VM, Yoo JU. In vitro chondrogenesis of bone marrow-derived mesenchymal progenitor cells. Exp Cell Res. 1998; 238(1):265–72. [PubMed: 9457080]
14. Muraglia A, Corsi A, Riminucci M, Mastrogiacomo M, Cancedda R, Bianco P, Quarto R. Formation of a chondro-osseous rudiment in micromass cultures of human bone-marrow stromal cells. J Cell Sci. 2003; 116(Pt 14):2949–55. [PubMed: 12783985]
15. Toh WS, Liu H, Heng BC, Rufaihah AJ, Ye CP, Cao T. Combined effects of TGFbeta1 and BMP2 in serum-free chondrogenic differentiation of mesenchymal stem cells induced hyaline-like cartilage formation. Growth Factors. 2005; 23(4):313–21. [PubMed: 16338794]
16. Puetzer JL, Petitte JN, Loboa EG. Comparative review of growth factors for induction of three-dimensional in vitro chondrogenesis in human mesenchymal stem cells isolated from bone marrow and adipose tissue. Tissue Eng Part B Rev. 2010; 16(4):435–44. [PubMed: 20196646]
17. Ma D, Ren L, Liu Y, Chen F, Zhang J, Xue Z, Mao T. Engineering scaffold-free bone tissue using bone marrow stromal cell sheets. J Orthop Res. 2010; 28(5):697–702. [PubMed: 19890976]
18. Murdoch AD, Grady LM, Ablett MP, Katopodi T, Meadows RS, Hardingham TE. Chondrogenic differentiation of human bone marrow stem cells in transwell cultures: generation of scaffold-free cartilage. Stem Cells. 2007; 25(11):2786–96. [PubMed: 17656642]
19. Mackay AM, Beck SC, Murphy JM, Barry FP, Chichester CO, Pittenger MF. Chondrogenic differentiation of cultured human mesenchymal stem cells from marrow. Tissue Eng. 1998; 4(4): 415–28. [PubMed: 9916173]
20. Renner JN, Kim Y, Liu JC. Bone morphogenetic protein-derived peptide promotes chondrogenic differentiation of human mesenchymal stem cells. Tissue Eng Part A. 2012; 18(23–24):2581–9. [PubMed: 22765926]
21. Schmitt B, Ringe J, Haupl T, Notter M, Manz R, Burmester GR, Sittinger M, Kaps C. BMP2 initiates chondrogenic lineage development of adult human mesenchymal stem cells in high-density culture. Differentiation. 2003; 71(9–10):567–77. [PubMed: 14686954]
22. Vanhatupa S, Ojansivu M, Autio R, Juntunen M, Miettinen S. Bone Morphogenetic Protein-2 Induces Donor-Dependent Osteogenic and Adipogenic Differentiation in Human Adipose Stem Cells. Stem Cells Transl Med. 2015; 4(12):1391–402. [PubMed: 26494778]
23. Tsumaki N, Yoshikawa H. The role of bone morphogenetic proteins in endochondral bone formation. Cytokine Growth Factor Rev. 2005; 16(3):279–85. [PubMed: 15869898]
24. Bianco P, Cancedda FD, Riminucci M, Cancedda R. Bone formation via cartilage models: the “borderline” chondrocyte. Matrix Biol. 1998; 17(3):185–92. [PubMed: 9707341]
25. Almubarak S, Nethercott H, Freeberg M, Beaudon C, Jha A, Jackson W, Marcucio R, Miclau T, Healy K, Bahney C. Tissue engineering strategies for promoting vascularized bone regeneration. Bone. 2016; 83:197–209. [PubMed: 26608518]
26. Scotti C, Tonnarelli B, Papadimitropoulos A, Scherberich A, Schaeren S, Schauerte A, Lopez-Rios J, Zeller R, Barbero A, Martin I. Recapitulation of endochondral bone formation using human adult mesenchymal stem cells as a paradigm for developmental engineering. Proc Natl Acad Sci U S A. 2010; 107(16):7251–6. [PubMed: 20406908]

27. Scotti C, Piccinini E, Takizawa H, Todorov A, Bourgine P, Papadimitropoulos A, Barbero A, Manz MG, Martin I. Engineering of a functional bone organ through endochondral ossification. Proc Natl Acad Sci U S A. 2013; 110(10):3997–4002. [PubMed: 23401508]
28. Mueller MB, Tuan RS. Functional characterization of hypertrophy in chondrogenesis of human mesenchymal stem cells. Arthritis Rheum. 2008; 58(5):1377–88. [PubMed: 18438858]
29. Farrell E, van der Jagt OP, Koevoet W, Kops N, van Manen CJ, Hellingman CA, Jahr H, O'Brien FJ, Verhaar JA, Weinans H, van Osch GJ. Chondrogenic priming of human bone marrow stromal cells: a better route to bone repair? Tissue Eng Part C Methods. 2009; 15(2):285–95. [PubMed: 19505182]
30. Freeman FE, Haugh MG, McNamara LM. Investigation of the optimal timing for chondrogenic priming of MSCs to enhance osteogenic differentiation in vitro as a bone tissue engineering strategy. J Tissue Eng Regen Med. 2016; 10(4):E250–62. [PubMed: 23922276]
31. Dang PN, Dwivedi N, Phillips LM, Yu X, Herberg S, Bowerman C, Solorio LD, Murphy WL, Alsberg E. Controlled Dual Growth Factor Delivery From Microparticles Incorporated Within Human Bone Marrow-Derived Mesenchymal Stem Cell Aggregates for Enhanced Bone Tissue Engineering via Endochondral Ossification. Stem Cells Transl Med. 2016; 5(2):206–17. [PubMed: 26702127]
32. Solorio LD, Dhami CD, Dang PN, Vieregge EL, Alsberg E. Spatiotemporal regulation of chondrogenic differentiation with controlled delivery of transforming growth factor-beta1 from gelatin microspheres in mesenchymal stem cell aggregates. Stem Cells Transl Med. 2012; 1(8): 632–9. [PubMed: 23197869]
33. Solorio LD, Phillips LM, McMillan A, Cheng CW, Dang PN, Samorezov JE, Yu X, Murphy WL, Alsberg E. Spatially organized differentiation of mesenchymal stem cells within biphasic microparticle-incorporated high cell density osteochondral tissues. Adv Healthc Mater. 2015; 4(15):2306–13. [PubMed: 26371790]
34. Solorio LD, Vieregge EL, Dhami CD, Dang PN, Alsberg E. Engineered cartilage via self-assembled hMSC sheets with incorporated biodegradable gelatin microspheres releasing transforming growth factor-beta1. J Control Release. 2012; 158(2):224–32. [PubMed: 22100386]
35. Dikina AD, Strobel HA, Lai BP, Rolle MW, Alsberg E. Engineered cartilaginous tubes for tracheal tissue replacement via self-assembly and fusion of human mesenchymal stem cell constructs. Biomaterials. 2015; 52:452–62. [PubMed: 25818451]
36. Solorio LD, Fu AS, Hernandez-Irizarry R, Alsberg E. Chondrogenic differentiation of human mesenchymal stem cell aggregates via controlled release of TGF-beta1 from incorporated polymer microspheres. J Biomed Mater Res A. 2010; 92(3):1139–44. [PubMed: 19322820]
37. Dang PN, Dwivedi N, Phillips LM, Bowerman C, Murphy WL, Alsberg E. Guiding chondrogenesis and osteogenesis with mineral-coated hydroxyapatite and BMP-2 incorporated within high-density hMSC aggregates for bone regeneration. ACS Biomater Sci Eng. 2016; 2(1): 30–42.
38. Dang SV, Phuong N, Herberg Davood, Hooman Riazi, Varghai Daniel, McMillan Alexandra, Awadallah Amad, Phillips Lauren M, Jeon Oju, Nguyen Minh K, Neha Dwivedi, Yu Xiaohua, Murphy William L, Alsberg Eben. Endochondral ossification in critical-sized bone defects via readily implantable scaffold-free stem cell constructs. Stem Cells Transl Med. 2017
39. Wegman F, Bijenhof A, Schuijff L, Oner FC, Dhert WJ, Alblas J. Osteogenic differentiation as a result of BMP-2 plasmid DNA based gene therapy in vitro and in vivo. Eur Cell Mater. 2011; 21:230–42. discussion 242. [PubMed: 21409753]
40. Raisin S, Belamie E, Morille M. Non-viral gene activated matrices for mesenchymal stem cells based tissue engineering of bone and cartilage. Biomaterials. 2016; 104:223–37. [PubMed: 27467418]
41. Saraf A, Mikos AG. Gene delivery strategies for cartilage tissue engineering. Adv Drug Deliv Rev. 2006; 58(4):592–603. [PubMed: 16766079]
42. Evans C. Using genes to facilitate the endogenous repair and regeneration of orthopaedic tissues. Int Orthop. 2014; 38(9):1761–9. [PubMed: 25038968]

43. Krebs MD, Salter E, Chen E, Sutter KA, Alsberg E. Calcium phosphate-DNA nanoparticle gene delivery from alginate hydrogels induces in vivo osteogenesis. J Biomed Mater Res A. 2010; 92(3):1131–8. [PubMed: 19322877]
44. Glover DJ, Lipps HJ, Jans DA. Towards safe, non-viral therapeutic gene expression in humans. Nat Rev Genet. 2005; 6(4):299–310. [PubMed: 15761468]
45. Southwood LL, Frisbie DD, Kawcak CE, McIlwraith CW. Delivery of growth factors using gene therapy to enhance bone healing. Vet Surg. 2004; 33(6):565–78. [PubMed: 15659011]
46. Gonzalez-Fernandez T, Sathy BN, Hobbs C, Cunniffe GM, McCarthy HO, Dunne NJ, Nicolosi V, O'Brien FJ, Kelly DJ. Mesenchymal Stem Cell Fate Following Non-viral Gene Transfection Strongly Depends on the Choice of Delivery Vector. Acta Biomater. 2017
47. Fang YL, Chen XG, TGW. Gene delivery in tissue engineering and regenerative medicine. J Biomed Mater Res B Appl Biomater. 2015; 103(8):1679–99. [PubMed: 25557560]
48. Xie Y, Yang ST, Kniss DA. Three-dimensional cell-scaffold constructs promote efficient gene transfection: implications for cell-based gene therapy. Tissue Eng. 2001; 7(5):585–98. [PubMed: 11694192]
49. Hosseinkhani H, Azzam T, Kobayashi H, Hiraoka Y, Shimokawa H, Domb AJ, Tabata Y. Combination of 3D tissue engineered scaffold and non-viral gene carrier enhance in vitro DNA expression of mesenchymal stem cells. Biomaterials. 2006; 27(23):4269–78. [PubMed: 16620957]
50. Lennon DP, Caplan AI. Isolation of human marrow-derived mesenchymal stem cells. Exp Hematol. 2006; 34(11):1604–5. [PubMed: 17046583]
51. Yu X, Khalil A, Dang PN, Alsberg E, Murphy WL. Multilayered Inorganic Microparticles for Tunable Dual Growth Factor Delivery. Adv Funct Mater. 2014; 24(20):3082–3093. [PubMed: 25342948]
52. Felka T, Schafer R, Schewe B, Benz K, Aicher WK. Hypoxia reduces the inhibitory effect of IL-1beta on chondrogenic differentiation of FCS-free expanded MSC. Osteoarthritis Cartilage. 2009; 17(10):1368–76. [PubMed: 19463979]
53. Adesida AB, Mulet-Sierra A, Jomha NM. Hypoxia mediated isolation and expansion enhances the chondrogenic capacity of bone marrow mesenchymal stromal cells. Stem Cell Res Ther. 2012; 3(2):9. [PubMed: 22385573]
54. Tiersch TR, Chandler RW, Wachtel SS, Elias S. Reference standards for flow cytometry and application in comparative studies of nuclear DNA content. Cytometry. 1989; 10(6):706–10. [PubMed: 2582960]
55. Sophia Fox AJ, Bedi A, Rodeo SA. The basic science of articular cartilage: structure, composition, and function. Sports Health. 2009; 1(6):461–8. [PubMed: 23015907]
56. Miao D, Scutt A. Histochemical localization of alkaline phosphatase activity in decalcified bone and cartilage. J Histochem Cytochem. 2002; 50(3):333–40. [PubMed: 11850436]
57. Riminucci M, Bradbeer JN, Corsi A, Gentili C, Descalzi F, Cancedda R, Bianco P. Vis-a-vis cells and the priming of bone formation. J Bone Miner Res. 1998; 13(12):1852–61. [PubMed: 9844103]
58. Azar, FM., Canale, ST., Beaty, JH., Campbell, WC. Campbell's operative orthopaedics. p. 1online resource
59. Barbara Young, P., BSc Med Sci (Hons), MB BChir, MRCP, FRCPA, O'Dowd, Geraldine, BSc (Hons), MBChB (Hons), FRCPath, Woodford, Phillip, MB BS, FRCPA. Skeletal Tissues. In: Young, B.O'Dowd, G., Woodford, P., editors. Wheater's functional histology : a text and colour atlas. 2014. p. ixp. 4331 online resource
60. Chan D, Jacenko O. Phenotypic and biochemical consequences of collagen X mutations in mice and humans. Matrix Biol. 1998; 17(3):169–84. [PubMed: 9707340]
61. Zara JN, Siu RK, Zhang X, Shen J, Ngo R, Lee M, Li W, Chiang M, Chung J, Kwak J, Wu BM, Ting K, Soo C. High doses of bone morphogenetic protein 2 induce structurally abnormal bone and inflammation in vivo. Tissue Eng Part A. 2011; 17(9–10):1389–99. [PubMed: 21247344]
62. Barradas AM, Monticone V, Hulsman M, Danoux C, Fernandes H, Tahmasebi Birgani Z, Barrere-de Groot F, Yuan H, Reinders M, Habibovic P, van Blitterswijk C, de Boer J. Molecular mechanisms of biomaterial-driven osteogenic differentiation in human mesenchymal stromal cells. Integr Biol (Camb). 2013; 5(7):920–31. [PubMed: 23752904]

63. He P, Sahoo S, Ng KS, Chen K, Toh SL, Goh JC. Enhanced osteoinductivity and osteoconductivity through hydroxyapatite coating of silk-based tissue-engineered ligament scaffold. J Biomed Mater Res A. 2013; 101(2):555–66. [PubMed: 22949167]
64. Suarez-Gonzalez D, Lee JS, Diggs A, Lu Y, Nemke B, Markel M, Hollister SJ, Murphy WL. Controlled multiple growth factor delivery from bone tissue engineering scaffolds via designed affinity. Tissue Eng Part A. 2014; 20(15–16):2077–87. [PubMed: 24350567]
65. Choi S, Murphy WL. Sustained plasmid DNA release from dissolving mineral coatings. Acta Biomater. 2010; 6(9):3426–35. [PubMed: 20304109]
66. Choi S, Yu X, Jongpaiboonkit L, Hollister SJ, Murphy WL. Inorganic coatings for optimized non-viral transfection of stem cells. Sci Rep. 2013; 3:1567. [PubMed: 23535735]
67. Lam AM, Cullis PR. Calcium enhances the transfection potency of plasmid DNA-cationic liposome complexes. Biochim Biophys Acta. 2000; 1463(2):279–90. [PubMed: 10675506]
68. Kyriakou CA, Yong KL, Benjamin R, Pizzey A, Dogan A, Singh N, Davidoff AM, Nathwani AC. Human mesenchymal stem cells (hMSCs) expressing truncated soluble vascular endothelial growth factor receptor (tsFlk-1) following lentiviral-mediated gene transfer inhibit growth of Burkitt's lymphoma in a murine model. J Gene Med. 2006; 8(3):253–64. [PubMed: 16288493]
69. Zayed M, Caniglia C, Misk N, Dhar MS. Donor-Matched Comparison of Chondrogenic Potential of Equine Bone Marrow- and Synovial Fluid-Derived Mesenchymal Stem Cells: Implications for Cartilage Tissue Regeneration. Front Vet Sci. 2016; 3:121. [PubMed: 28149840]
70. Phinney DG, Kopen G, Righter W, Webster S, Tremain N, Prockop DJ. Donor variation in the growth properties and osteogenic potential of human marrow stromal cells. J Cell Biochem. 1999; 75(3):424–36. [PubMed: 10536366]
71. Scharstuhl A, Schewe B, Benz K, Gaissmaier C, Buhring HJ, Stoop R. Chondrogenic potential of human adult mesenchymal stem cells is independent of age or osteoarthritis etiology. Stem Cells. 2007; 25(12):3244–51. [PubMed: 17872501]
72. Yu X, Murphy WL. 3-D Scaffold Platform for Optimized Non-viral Transfection of Multipotent Stem Cells. J Mater Chem B Mater Biol Med. 2014; 2(46):8186–8193. [PubMed: 25541592]
73. Macri L, Silverstein D, Clark RA. Growth factor binding to the pericellular matrix and its importance in tissue engineering. Adv Drug Deliv Rev. 2007; 59(13):1366–81. [PubMed: 17916397]
74. Zhu Y, Oganesian A, Keene DR, Sandell LJ. Type IIA procollagen containing the cysteine-rich amino propeptide is deposited in the extracellular matrix of prechondrogenic tissue and binds to TGF-beta1 and BMP-2. J Cell Biol. 1999; 144(5):1069–80. [PubMed: 10085302]
75. Hynes RO. The extracellular matrix: not just pretty fibrils. Science. 2009; 326(5957):1216–9. [PubMed: 19965464]
76. Hyytiainen M, Penttinen C, Keski-Oja J. Latent TGF-beta binding proteins: extracellular matrix association and roles in TGF-beta activation. Crit Rev Clin Lab Sci. 2004; 41(3):233–64. [PubMed: 15307633]
77. Fierro FA, Kalomoiris S, Sondergaard CS, Nolta JA. Effects on proliferation and differentiation of multipotent bone marrow stromal cells engineered to express growth factors for combined cell and gene therapy. Stem Cells. 2011; 29(11):1727–37. [PubMed: 21898687]
78. Miyazono K. Positive and negative regulation of TGF-beta signaling. J Cell Sci. 2000; 113(Pt 7): 1101–9. [PubMed: 10704361]
79. Jilka RL, Weinstein RS, Bellido T, Parfitt AM, Manolagas SC. Osteoblast programmed cell death (apoptosis): modulation by growth factors and cytokines. J Bone Miner Res. 1998; 13(5):793–802. [PubMed: 9610743]
80. Ishaug-Riley SL, Crane-Kruger GM, Yaszemski MJ, Mikos AG. Three-dimensional culture of rat calvarial osteoblasts in porous biodegradable polymers. Biomaterials. 1998; 19(15):1405–12. [PubMed: 9758040]
81. Wang EA, Rosen V, D'Alessandro JS, Bauduy M, Cordes P, Harada T, Israel DI, Hewick RM, Kerns KM, LaPan P, et al. Recombinant human bone morphogenetic protein induces bone formation. Proc Natl Acad Sci U S A. 1990; 87(6):2220–4. [PubMed: 2315314]

82. Madeira C, Mendes RD, Ribeiro SC, Boura JS, Aires-Barros MR, da Silva CL, Cabral JM. Nonviral gene delivery to mesenchymal stem cells using cationic liposomes for gene and cell therapy. J Biomed Biotechnol. 2010; 2010:735349. [PubMed: 20625411]

## Significance statement

This work describes a novel approach to non-viral delivery of plasmid DNA (pDNA) encoding therapeutic growth factors from microparticles embedded within scaffold-free, mesenchymal stem cell (MSC) condensations for osseous tissue formation and repair of bone defects. Local presentation of transgenes from the microparticles can instruct MSC differentiation down chondrogenic and/or osteogenic lineages, avoiding the need for repeat exogenous supplementation with recombinant growth factors for a more rapidly implantable regenerative therapy. MSC donor variability in differentiation response to growth factor-encoded pDNA suggests the need to screen individual patient's MSCs with the inductive factors prior to clinical implementation. The work presented here is an important step in the engineering of a high-density stem cell system with incorporated instructive genetic cues for regeneration of bone and other tissues.

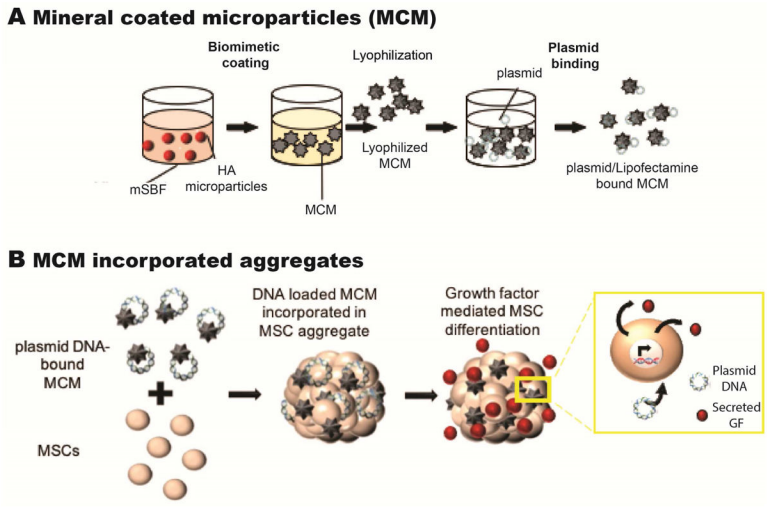


**Figure 1.**

A) Schematic showing MCM synthesis and plasmid DNA binding to MCM. B) Schematic of plasmid DNA-bound MCM incorporation into an MSC aggregate.

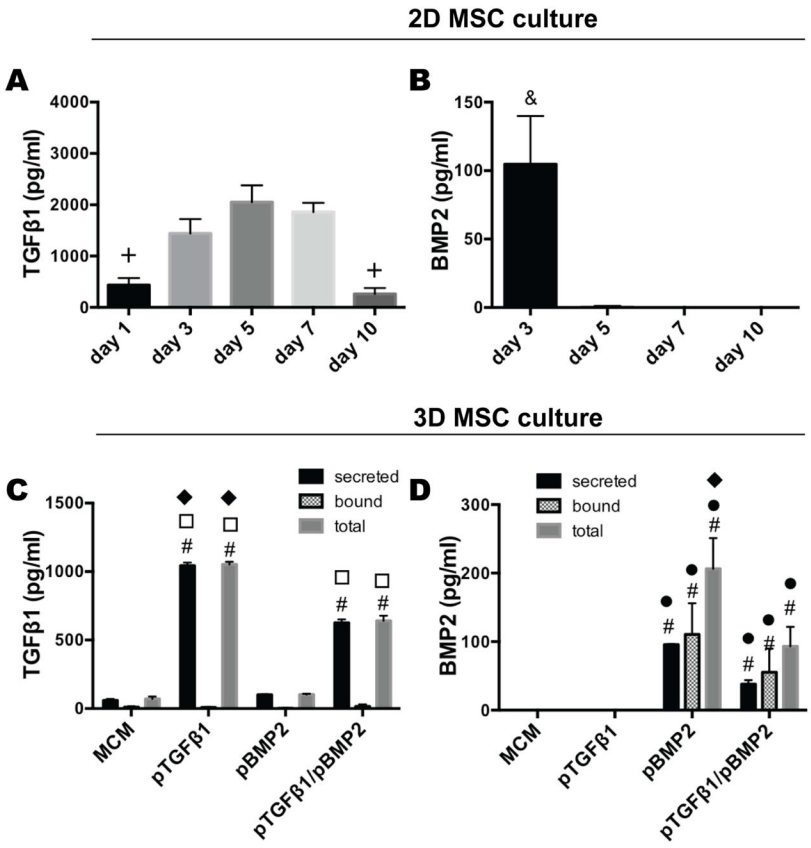


**Figure 2.**

Transgene-mediated GF production in 2D and 3D MSC culture. A) TGF-β1 and B) BMP-2 production from pTGF-β1 and pBMP-2 treated monolayer MSCs, respectively, over time. C) TGF-β1 and D) BMP-2 production from 3D MSC aggregates containing MCM alone (MCM), pTGF-β1, pBMP-2, and pTGF-β1/pBMP-2 after 3 days in vitro culture. Growth factor secretion into the culture medium (secreted) and bound within the aggregate (bound) was quantified. The sum of the secreted and bound growth factor is represented as the total growth factor (total). + denotes significance in comparison to days 3, 5, and 7, & in comparison to all other time points, # in comparison to aggregates containing MCM alone, ● in comparison to pTGFβ1, □ in comparison to pBMP2, and ◆ in comparison to pTGFβ1/pBMP2 ($p<0.05$). MCM, mineral-coated hydroxyapatite microparticles; TGFβ1, transforming growth factor-beta 1; BMP2, bone morphogenetic protein-2.

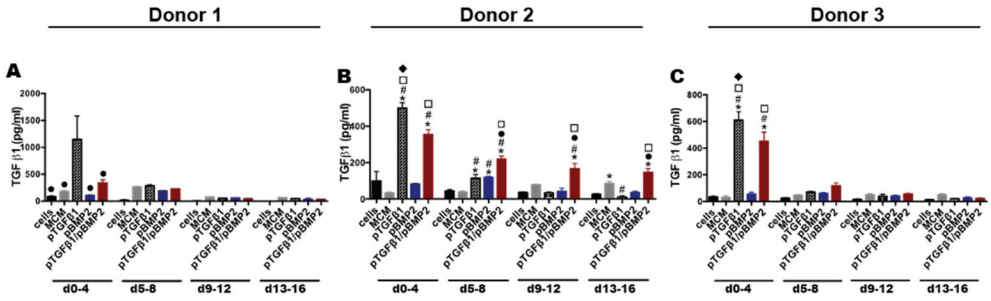


**Figure 3.**

Time course of TGF-β1 production from MSC aggregates cultured with microparticle-loaded transgenes. Secreted TGF-β1 over time from **Donor** A) **1**, B) **2**, and C) **3** aggregates over 16 days in vitro culture. * denotes significance in comparison to cells, # in comparison to MCM, ● in comparison to pTGFβ1, □ in comparison to pBMP2, and ◆ in comparison to pTGFβ1/pBMP2, ($p<.05$). MCM, mineral-coated hydroxyapatite microparticles; TGFβ1, transforming growth factor-beta 1; BMP2, bone morphogenetic protein-2.

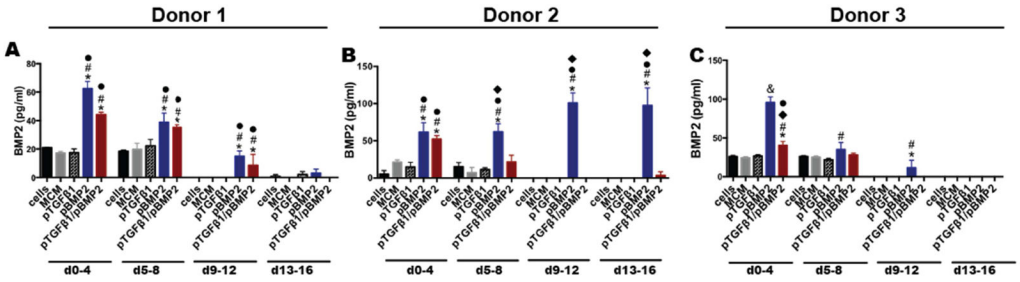


**Figure 4.**

Time course of BMP-2 production from MSC aggregates cultured with microparticle-loaded transgenes. Secreted BMP-2 over time from **Donor** A) **1**, B) **2**, and C) **3** aggregates over 16 days in vitro culture. * denotes significance in comparison to cells, # in comparison to MCM, ● in comparison to pTGFβ1, □ in comparison to pBMP2, and ◆ in comparison to pTGFβ1/pBMP2, ($p<.05$). MCM, mineral-coated hydroxyapatite microparticles; TGFβ1, transforming growth factor-beta 1; BMP2, bone morphogenetic protein-2.

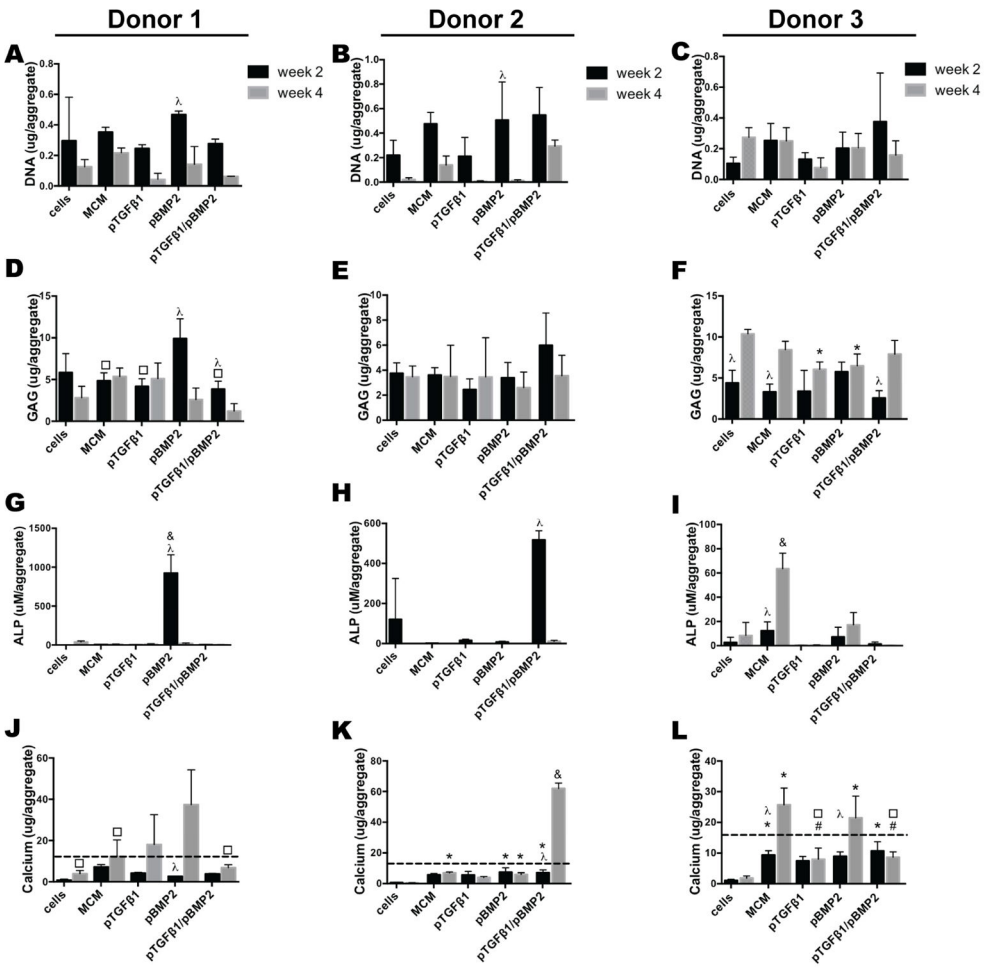


**Figure 5.**

Biochemical analysis of MSC aggregates from three donors cultured with incorporated microparticle-loaded transgenes. A–C) DNA content, D–F) GAG content, G–I) ALP activity, and J–L) calcium content of **Donor 1, 2, and 3** aggregates after 2 and 4 weeks in vitro culture. The dashed line in J, K, and L indicates the amount of calcium initially incorporated into aggregates from MCM-derived calcium, assuming 100% incorporation efficiency. * denotes significance in comparison to cells, # in comparison to MCM, ● in comparison to pTGFβ1 aggregates, □ in comparison to pBMP2, & in comparison to all other groups, and **λ** for comparison between timepoints within a condition, ($p<0.05$). ALP, alkaline phosphatase; GAG, glycosaminoglycan; MCM, mineral-coated hydroxyapatite microparticles; TGFβ1, transforming growth factor-beta 1; BMP2, bone morphogenetic protein-2.

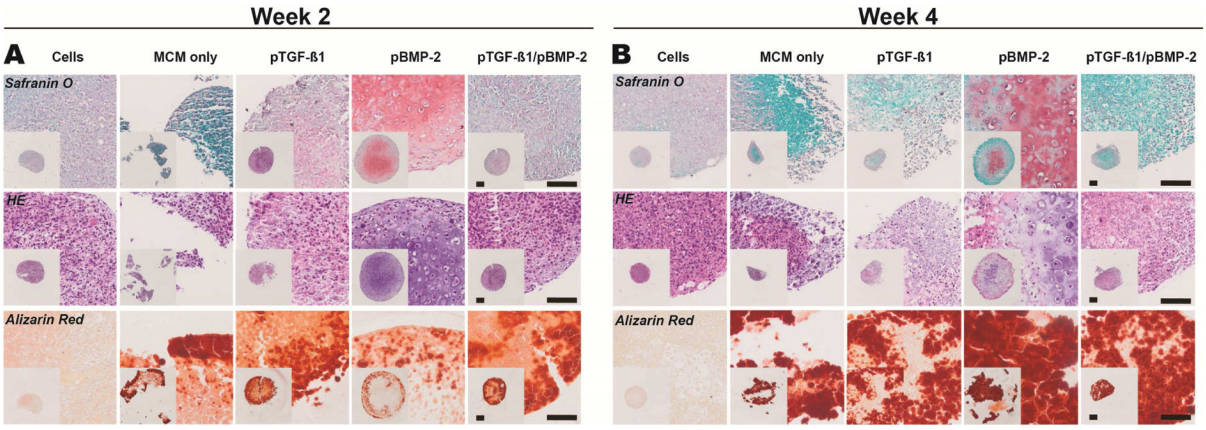


**Figure 6.**

Histologic characterization of **Donor 1** MSC aggregates with incorporated microparticle-loaded transgenes. Tissue sections were stained with Safranin O for GAG (pink/red), hematoxylin and eosin, and Alizarin Red (red) for calcium after A) 2 and B) 4 weeks in vitro culture. HE, Hematoxylin and Eosin; MCM, mineral coated hydroxyapatite microparticles; TGFβ1, transforming growth factor-beta 1; BMP2, bone morphogenetic protein-2. Scale bars, 100 μm.

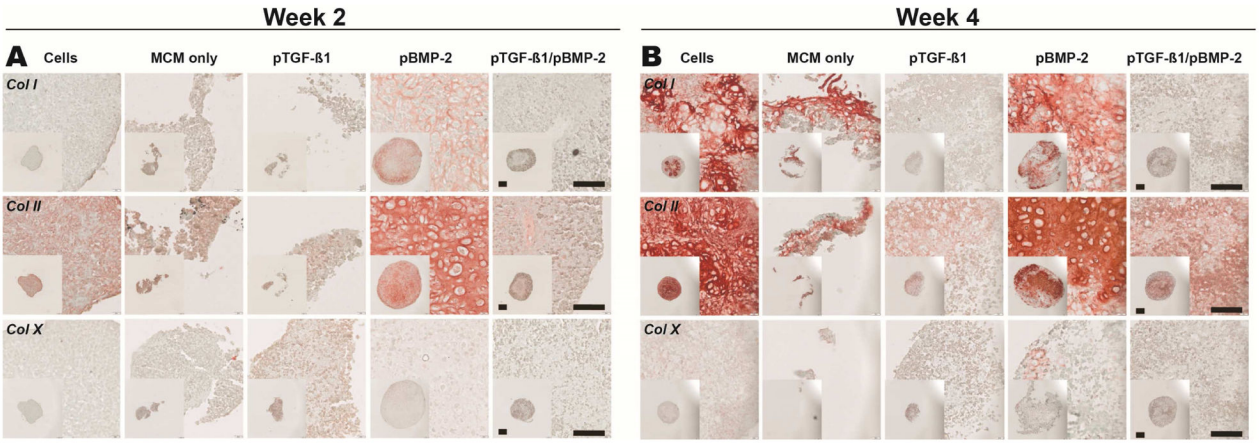


**Figure 7.**

Immunohistochemical characterization of **Donor 1** MSC aggregates with incorporated microparticle-loaded transgenes. Tissue sections were stained for col I, II, and X (pink/red) with Fast Green Counterstain after A) 2 weeks and B) 4 weeks in vitro culture. Col I, collagen type I; Col II, collagen type II; Col X, collagen type X; MCM, mineral-coated hydroxyapatite microparticles; TGFβ1, transforming growth factor-beta 1; BMP2, bone morphogenetic protein-2. Scale bars, 100 μm.